

# Introduction to the Spectrum of $\mathcal{N} = 4$ SYM and the Quantum Spectral Curve

Nikolay Gromov

Mathematics Department, King's College London, The Strand, London WC2R 2LS, UK.  
& St.Petersburg INP, Gatchina, 188 300, St.Petersburg, Russia

**Abstract.** *This review is based on the lectures given by the author at the Les Houches Summer School 2016. It describes the recently developed Quantum Spectral Curve (QSC) for a non-perturbative planar spectrum of  $N=4$  Super Yang-Mills theory in a pedagogical way starting from the harmonic oscillator and avoiding a long historical path. We give many examples and provide exercises. At the end we give a list of the recent and possible future applications of the QSC.*

**Dedication.** In memory of Ludvig Dmitrievich Faddeev.



# Contents

<b>1</b>	<b>Introduction</b>	<b>5</b>
<b>2</b>	<b>From Harmonic Oscillator to QQ-Relations</b>	<b>7</b>
2.1	Inspiration from the Harmonic Oscillator . . . . .	7
2.2	$SU(2)$ -Heisenberg Spin Chain . . . . .	9
2.3	Nested Bethe Ansatz and $QQ$ -relations . . . . .	11
2.3.1	Bosonic duality . . . . .	12
2.3.2	Fermionic duality in $SU(N M)$ . . . . .	16
2.4	$QQ$ -relations for $PSU(2, 2 4)$ Spin Chain . . . . .	18
<b>3</b>	<b>Classical String and Strong Coupling Limit of QSC</b>	<b>23</b>
3.1	Classical String Action . . . . .	23
3.2	Classical Integrability . . . . .	24
3.3	Quasimomenta and the Strong Coupling Limit of QSC . . . . .	27
<b>4</b>	<b>QSC Formulation</b>	<b>29</b>
4.1	Main $QQ$ -Relations . . . . .	29
4.2	Large $u$ Asymptotic and the Quantum Numbers of the State . . . . .	30
4.3	Analytic Structure of $Q$ -functions . . . . .	31
4.4	Gluing Conditions . . . . .	33
4.5	Left-Right Symmetric Sub-Sector . . . . .	34
<b>5</b>	<b>QSC - analytic examples</b>	<b>35</b>
5.1	$sl(2)$ Sector . . . . .	35
5.2	Analytic Continuation in $S$ . . . . .	36
5.3	Slope Function . . . . .	38
<b>6</b>	<b>Solving QSC at finite coupling Numerically</b>	<b>43</b>
6.1	Description of the Method . . . . .	43
6.2	Implementation in <i>Mathematica</i> . . . . .	45
<b>7</b>	<b>Applications, Further Reading and Open Questions</b>	<b>49</b>

Bibliography

53

# Introduction

The importance of AdS/CFT correspondence in modern theoretical physics and the role of  $\mathcal{N} = 4$  SYM in it is hard to over-appreciate. In these lecture notes we try to give a pedagogical introduction to the Quantum Spectral Curve (QSC) of  $\mathcal{N} = 4$  SYM, a beautiful mathematical structure which describes the non-perturbative spectrum of strings/anomalous dimensions of all single trace operators. The historical development leading to the discovery of the QSC [7, 11] is a very long and interesting story by itself, and there are several reviews trying to cover the main steps on this route [6, 18]. For the purposes of the lectures we took another approach and try to motivate the construction by emphasizing numerous analogies between the QSC construction and basic quantum integrable systems such as the harmonic oscillator, Heisenberg spin chains, and classical sigma-models. In this way the QSC comes out naturally, bypassing extremely complicated and technical stages such as derivation of the S-matrix [19], dressing phase [20], mirror theory [22], Y-system [2], Thermodynamic Bethe Ansatz [3, 24, 25, 23], NLIE [7, 26] and finally derivation of the QSC [7, 11].

We also give examples of analytic solutions of the QSC and in the last chapter describe step-by-step the numerical algorithm allowing us to get the non-perturbative spectrum with almost unlimited precision [13]. We also briefly discuss the analytic continuation of the anomalous dimension to the Regge (BFKL) limit relevant for more realistic QCD.

The structure is the following: in the Chapter 1 we re-introduce the harmonic oscillator and the Heisenberg spin chains in a way suitable for generalization to the QSC. Chapter 2 describes classical integrability of strings in a curved background, which give some important hints about the construction of the QSC. In Chapter 3 we give a clear formulation of the QSC. In Chapter 4 we consider some analytic examples. And in the last Chapter 5 we present the numerical method.

**Acknowledgment** I am very grateful to M.Alfimov, A.Cavaglià, S.Leurent, F.Levkovich-Malyuk, G.Sizov, D.Volin, and especially to V.Kazakov and P.Vieira for numerous discussions on closely related topics. I am thankful to D.Grabner, D.Lee and J.<sup>1</sup> for carefully reading the manuscript. The work was supported by the European Research Council (Programme “Ideas” ERC-2012-AdG 320769 AdS-CFT-solvable). We are grateful to Humboldt University (Berlin) for the hospitality and financial support of this work in the framework of the “Kosmos” programme. We wish to thank STFC for support from Consolidated grant number ST/J002798/1. This work has received funding from the People Programme (Marie Curie Actions) of the European Union’s Seventh Framework Programme FP7/2007-2019/ under REA Grant Agreement No 317089 (GATIS).

Please report typos or send other improvement requests for these lecture notes to [nikgromov@gmail.com](mailto:nikgromov@gmail.com).

---

<sup>1</sup>i.e. Julius, who only has a first name

# From Harmonic Oscillator to QQ-Relations

## 2.1 Inspiration from the Harmonic Oscillator

To motivate the construction of the QSC we first consider the 1D harmonic oscillator and concentrate on the features which, as we will see later, have similarities with the construction for the spectrum of  $\mathcal{N} = 4$  SYM.

The harmonic oscillator is the simplest integrable model which at the same time exhibits nontrivial features surprisingly similar to  $\mathcal{N} = 4$  SYM. Our starting point is the Schrödinger equation

$$-\frac{\hbar^2}{2m}\psi''(x) + V(x)\psi(x) = E\psi(x) \quad (2.1)$$

where  $V(x) = \frac{m\omega^2 x^2}{2}$ . Alternatively, it can be written in terms of the quasi-momentum

$$p(x) = \frac{\hbar \psi'(x)}{i \psi(x)} \quad (2.2)$$

as

$$p^2 - i\hbar p' = 2m(E - V) . \quad (2.3)$$

This non-linear equation is completely equivalent to (2.1). Instead of solving this equation directly let us make a simple ansatz for  $p(x)$ . We see that for large  $x$  the r.h.s. behaves as  $-m^2\omega^2 x^2$  implying that at infinity  $p \simeq im\omega x$ . Furthermore,  $p(x)$  should have simple poles at the position of zeros of the wave function which we denote  $x_i$ . All the residues at these points should be equal to  $\hbar/i$  as one can see from (2.2). We can accommodate all these basic analytical properties with the following ansatz:

$$p(x) = im\omega x + \frac{\hbar}{i} \sum_{i=1}^N \frac{1}{x - x_i} . \quad (2.4)$$

We note that at large  $x$  the r.h.s. of (2.4) behaves as  $im\omega x + \frac{\hbar}{i} \frac{N}{x} + O(1/x^2)$ . Plugging this large  $x$  approximation of  $p(x)$  into the exact equation (2.3) we get:

$$\left( im\omega x + \frac{\hbar}{i} \frac{N}{x} \right)^2 + \hbar(m\omega) = 2m(E - m^2\omega^2 x^2/2) + O(1/x) . \quad (2.5)$$

Comparing the coefficients in front of  $x^2$  and  $x^0$  we get  $E = \hbar\omega(N+1/2)$  which is the famous formula for the spectrum of the harmonic oscillator. In order to reconstruct the wave function we expand (2.3) near the pole  $x = x_i$ . Namely, we require

$$\text{res}_{x=x_k} \left[ \left( im\omega x + \frac{\hbar}{i} \sum_{i=1}^N \frac{1}{x-x_i} \right)^2 + i\hbar \frac{\hbar}{i} \sum_{i=1}^N \frac{1}{(x-x_i)^2} \right] = 0, \quad (2.6)$$

obtaining (from the first bracket)

$$x_k = \frac{\hbar}{\omega m} \sum_{j \neq i}^N \frac{1}{x_i - x_k}, \quad k = 1, \dots, N. \quad (2.7)$$

This set of equations determines all  $x_k$  in a unique way.

---

**Exercise 1.** Verify for 1 and 2 roots that there is a unique up to a permutation solution of the equation (2.7), find the solution.

---

Finally, we can integrate (2.2) to obtain

$$\psi(x) = e^{-\frac{m\omega x^2}{2\hbar}} Q(x), \quad Q(x) \equiv \prod_{i=1}^N (x - x_i). \quad (2.8)$$

It is here for the first time we see the Q-function, which is the analog of the main building block of the QSC! We will refer to equation (2.7) for zeros of the Q-functions as the Bethe ansatz equation. We will call  $\{x_i\}$  the Bethe roots.

Let us outline the main features which will be important for what follows:

- The asymptotic of  $Q(x) \sim x^N$  contains quantum numbers of the state.
- Zeros of the  $Q(x)$  function can be determined from the condition of cancellation of poles (2.6) (analog of Baxter equation) which can be explicitly written as (2.7) (analog of Bethe equations).
- The wave function can be completely determined from the Bethe roots or from  $Q(x)$  (by adding a simple universal for all states factor).
- The Schrödinger equation has a second (non-normalizable) solution which behaves as  $\psi_2 \simeq x^{-N-1} e^{+\frac{m\omega}{2\hbar} x^2}$ . Together with the normalizable solution  $\psi_1$  they form a Wronskian

$$W = \begin{vmatrix} \psi_1(x) & \psi_1'(x) \\ \psi_2(x) & \psi_2'(x) \end{vmatrix} \quad (2.9)$$

which is a constant.

---

**Exercise 2.** Prove that the Wronskian  $W$  is a constant for a general Schrödinger equation.

---



## 2.2 $SU(2)$ -Heisenberg Spin Chain

In this section we discuss how the construction from the previous section generalizes to integrable spin chains – a system with a large number of degrees of freedom. The simplest spin chain is the Heisenberg  $SU(2)$  magnetic which is discussed in great detail in numerous reviews and lectures. We highly recommend Faddeev’s 1982 Les Houches lectures [27] for that. We describe the results most essential for us below.

In short, the Heisenberg spin chain is a chain of  $L$  spin-1/2 particles with a nearest neighbour interaction. The Hamiltonian of the system can be written as

$$\hat{H} = 2g^2 \sum_{i=1}^L (1 - P_{i,i+1}) \quad (2.10)$$

where  $P_{i,i+1}$  is an operator which permutes the particles at the position  $i$  and  $i + 1$  and  $g$  is a constant. We introduce twisted boundary conditions by defining

$$P_{L,L+1} |\uparrow, \dots, \uparrow\rangle = |\uparrow, \dots, \uparrow\rangle, \quad P_{L,L+1} |\uparrow, \dots, \downarrow\rangle = e^{+2i\phi} |\downarrow, \dots, \uparrow\rangle, \quad (2.11)$$

$$P_{L,L+1} |\downarrow, \dots, \downarrow\rangle = |\downarrow, \dots, \downarrow\rangle, \quad P_{L,L+1} |\downarrow, \dots, \uparrow\rangle = e^{-2i\phi} |\uparrow, \dots, \downarrow\rangle. \quad (2.12)$$

The states can, again, be described by the Baxter function  $Q_1(u) = e^{\phi u} \prod_{i=1}^{N_1} (u - u_i)$ . The Bethe roots  $u_i$  have a physical meaning – they represent the momenta  $p_i$  of spin down “excitations” moving in a sea of spin ups via  $u_i = \frac{1}{2} \cot \frac{p_i}{2}$  (see Fig.2.1). We find the roots  $u_j$  from the equation similar to (2.7)<sup>1</sup>

$$\left( \frac{u_k + i/2}{u_k - i/2} \right)^L = e^{-2i\phi} \prod_{j \neq k}^{N_1} \frac{u_k - u_j + i}{u_k - u_j - i}, \quad k = 1, \dots, N_1 \quad (2.13)$$

---

**Exercise 3.** Take log and expand for large  $u_k$ . You should get exactly the same as (2.7) up to a rescaling and shift of  $u_j$ .

---

from where one gets a discrete set of solutions for  $\{u_i\}$ . The energy is then given by

$$E = \sum_j^{N_1} \frac{2g^2}{u_j^2 + 1/4}. \quad (2.14)$$

---

**Exercise 4.** Take  $L = 2$  and compute the energy spectrum in two different ways: 1) by directly diagonalizing the Hamiltonian (2.10), which becomes a  $4 \times 4$  matrix of the form

$$2g^2 \begin{pmatrix} 0 & 0 & 0 & 0 \\ 0 & 2 & -1 - e^{-2i\phi} & 0 \\ 0 & -1 - e^{2i\phi} & 2 & 0 \\ 0 & 0 & 0 & 0 \end{pmatrix}$$

Next solve the Bethe equation (2.13) for  $N_1 = 0, 1, 2$  and compute the energy from the formula (2.14).

---

<sup>1</sup>One should assume all  $u_j$  to be different like in the harmonic oscillator case.

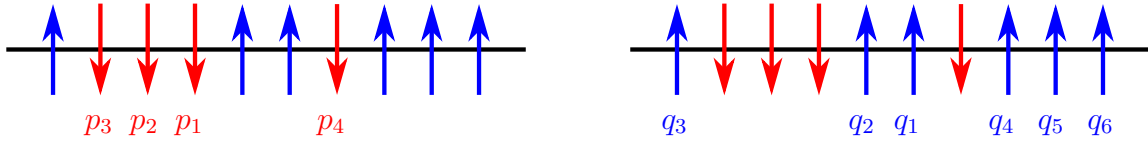


**Figure 2.1:** Two equivalent representations of the same state. In the first case we treat spin downs as excitations (magnons) moving with some momenta  $p_i$  and all spin ups correspond to the reference (vacuum) state. In the second case we treat spin ups as excitations moving with some momenta  $q_i$ .

One could ask what the analog of the Schrödinger equation is in this case. The answer is given by the Baxter equation of the form

$$T(u)Q_1(u) = (u + i/2)^L Q_1(u - i) + (u - i/2)^L Q_1(u + i), \quad (2.15)$$

where  $T(u)$  is a polynomial which plays the role of the potential, but it is not fixed completely and has to be determined from the self-consistency of (2.15).

---

**Exercise 5.** Show that the leading large  $u$  coefficients of  $T(u)$  are  $T(u) \simeq 2 \cos \phi u^L + u^{L-1}(N_2 - N_1) \sin \phi$  where  $N_2 = L - N_1$ .

---

In practice we do not even need to know  $T(u)$  as it is sufficient to require polynomiality from  $T(u)$  to get (2.13) as a condition of cancellation of the poles.

---

**Exercise 6.** For generic polynomial  $Q(u)$  we see that  $T(u)$  is a rational function with poles at  $u = u_k$ , where  $Q(u_k) = 0$ . Show that these poles cancel if the Bethe ansatz equation (2.13) is satisfied.

---

Notice that given some polynomial  $T(u)$  there is another polynomial (up to a  $e^{-u\phi}$  multiplier to “twist”  $\phi$ ) solution to the Baxter equation, just like we had before for the Schrödinger equation. Its asymptotics are  $Q_2 \simeq e^{-u\phi} u^{N_2}$  where  $N_2 = L - N_1$ . The roots of  $Q_2$  also has a physical interpretation – they describe the  $L - N_1$  spin up particles moving in the sea of the spin downs (i.e. opposite to  $Q_1$  which described the reflected picture where the spin ups played the role of the observers and the spin-downs were considered as particles). The second solution together with the initial one should satisfy the Wronskian relation (in the same way as for the Schrödinger equation)<sup>2</sup>

$$\begin{vmatrix} Q_1(u - i/2) & Q_1(u + i/2) \\ Q_2(u - i/2) & Q_2(u + i/2) \end{vmatrix} \propto Q_{12}(u) \quad (2.16)$$

where  $Q_{12}(u)$  satisfies

$$\frac{Q_{12}(u + i/2)}{Q_{12}(u - i/2)} = \frac{(u + i/2)^L}{(u - i/2)^L} \quad (2.17)$$

so we conclude that  $Q_{12}(u) = -2i \sin \phi u^L$ .

---

<sup>2</sup>The  $\propto$  sign is used to indicate that the equality holds up to a numerical multiplier (which can be easily recovered from large  $u$  limit).

---

**Exercise 7.** Show that if  $Q_1$  and  $Q_2$  are two linearly independent solutions of (2.15), then (2.17) holds.

---

We see that there are strict similarities with the harmonic oscillator. Furthermore, it is possible to invert the above logic and prove the following statement: equation (2.16) plus the polynomiality assumption (up to an exponential prefactor) by itself implies the Bethe equation, from which we departed. This logic is very close to the philosophy of the QSC.

---

**Exercise 8.** Show that the Baxter equation is the following “trivial” statement

---

$$\begin{vmatrix} Q(u-i) & Q(u) & Q(u+i) \\ Q_1(u-i) & Q_1(u) & Q_1(u+i) \\ Q_2(u-i) & Q_2(u) & Q_2(u+i) \end{vmatrix} = 0 \quad , \quad \text{for } Q = Q_1 \text{ or } Q = Q_2 . \quad (2.18)$$

From that determine  $T(u)$  in terms of  $Q_1$  and  $Q_2$ .

---

## 2.3 Nested Bethe Ansatz and QQ-relations

The symmetry of the Heisenberg spin chain from the previous section is  $SU(2)$ . In order to get closer to  $PSU(2, 2|4)$  (the symmetry of  $\mathcal{N} = 4$  SYM) we now consider a generalization of the Heisenberg spin chain for the  $SU(3)$  symmetry group. For that we just have to assume that there are 3 possible states per chain site instead of 2, otherwise the construction of the Hamiltonian is very similar.

The spectrum of the  $SU(3)$  spin chain can be found from the “Nested” Bethe ansatz equations [28], which now involve two different unknown (twisted) polynomials  $Q_A$  and  $Q_B$ . They can be written as<sup>3</sup>:

$$\begin{aligned} 1 &= -\frac{Q_A^{++}Q_B^-}{Q_A^{--}Q_B^+} \quad , \quad u = u_{A,i} \\ \frac{Q_\theta^+}{Q_\theta^-} &= -\frac{Q_A^-Q_B^{++}}{Q_A^+Q_B^{--}} \quad , \quad u = u_{B,i} \end{aligned} \quad (2.19)$$

and the energy is given by

$$E = i\partial_u \log \frac{Q_B^+}{Q_B^-} \Big|_{u=0} . \quad (2.20)$$

We denote  $Q_\theta = u^L$ . We also introduced some very convenient notation

$$f^\pm = f(u \pm i/2) \quad , \quad f^{\pm\pm} = f(u \pm i) \quad , \quad f^{[\pm a]} = f(u \pm ai/2). \quad (2.21)$$

---

**Exercise 9.** Show that the  $SU(3)$  Bethe equations reduce to the  $SU(2)$  equations (2.13) and (2.14) when  $Q_A = 1$ .

---

<sup>3</sup>by the twisted polynomials we mean the functions of the form  $e^{\psi u} \prod_i (u - u_i)$ , for some number  $\psi$ .

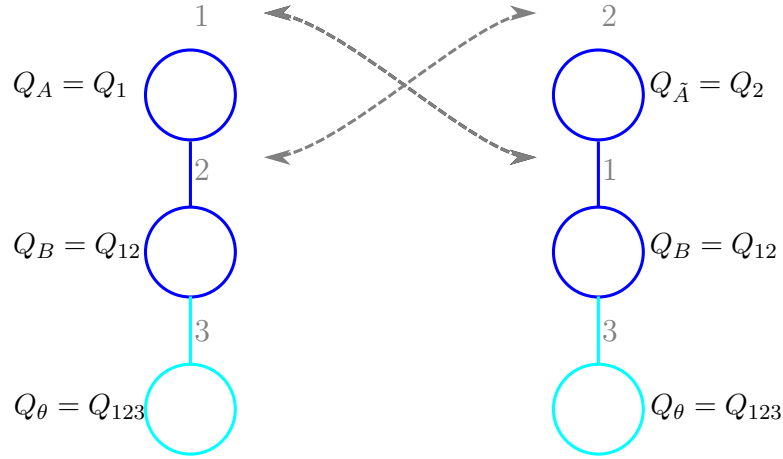


**Figure 2.2:** Bosonic duality applied to the first node of the BA.

### 2.3.1 Bosonic duality

From the  $SU(2)$  Heisenberg spin chain we learned that the Baxter polynomial  $Q_1(u)$  contains as many roots as arrow-downs we have in our state. In particular the trivial polynomial  $Q_1(u) = e^{-u\phi}$  corresponds to the state  $|\uparrow\uparrow\dots\uparrow\rangle$ . One can also check that there is only one solution of the Bethe equations where  $Q_1(u)$  is a twisted polynomial of degree  $L$  and it satisfies

$$e^{i\phi/2}Q_1^- - e^{-i\phi/2}Q_1^+ = 2i \sin \phi u^L e^{-u\phi} . \quad (2.22)$$

**Exercise 10.** Solve this equation for  $L = 1$  and  $L = 2$  and check that  $Q_1$  also solves the Bethe equations of the  $SU(2)$  spin chain. Compute the corresponding energy.

As this equation produces a polynomial of degree  $L$  it must correspond to the maximally “excited” state  $|\downarrow\downarrow\dots\downarrow\rangle$ . It is clear that even though physically these states are very similar our current description in terms of the Bethe ansatz singles out one of them. We will see that there is a “dual” description where the  $Q$ -function corresponding to the state  $|\downarrow\downarrow\dots\downarrow\rangle$  is trivial. In the case of the  $SU(3)$  spin chain where we have 3 different states per node of the spin chain, which we can denote 1, 2, 3, there are 3 equivalent vacuum states  $|11\dots 1\rangle$ ,  $|22\dots 2\rangle$ , and  $|33\dots 3\rangle$ , but only one of them corresponds to the trivial solution of the  $SU(3)$  nested Bethe ansatz. Below we concentrate on the  $SU(3)$  case and demonstrate that there are several equivalent sets of Bethe ansatz equations (2.19).

To build a dual set of Bethe equations we first have to pick a  $Q$ -function which we are going to dualise. For example we can build a new set of Bethe equations by replacing  $Q_A$ , a twisted polynomial of degree  $N_A$ , with another twisted polynomial  $Q_{\bar{A}}$  of degree  $N_{\bar{A}} = N_B - N_A$ , where  $N_B$  is the degree of the polynomial  $Q_B$ . For that we find a dual  $Q$ -function  $Q_{\bar{A}}$  from

$$\begin{vmatrix} Q_A^- & Q_A^+ \\ Q_{\bar{A}}^- & Q_{\bar{A}}^+ \end{vmatrix} \propto Q_B(u) . \quad (2.23)$$

Let's see that  $Q_{\tilde{A}}$  satisfies the same Bethe equation. By evaluating (2.23) at  $u = u_{\tilde{A},i} + i/2$  and dividing by the same relation evaluated at  $u = u_{\tilde{A},i} - i/2$  we get:

$$\frac{Q_A Q_{\tilde{A}}^{++} - 0}{0 - Q_A Q_{\tilde{A}}^{--}} = \frac{Q_B^+}{Q_B^-}, \quad u = u_{\tilde{A},i} \quad (2.24)$$

which is exactly the first equation (2.19) with  $A$  replaced by  $\tilde{A}$ ! To accomplish our goal we should also exclude  $Q_A$  from the second equation. For that we notice that at  $u = u_{B,i}$  the relation gives

$$\frac{Q_A^-}{Q_A^+} = \frac{Q_{\tilde{A}}^-}{Q_{\tilde{A}}^+}, \quad u = u_{B,i} \quad (2.25)$$

which allows us to rewrite the whole set of equations (2.19) in terms of  $Q_{\tilde{A}}$ . We call this transformation a Bosonic duality. Similarly one can apply the dualization procedure to  $Q_B$ . We determine  $Q_{\tilde{B}}$  from

$$\begin{vmatrix} Q_B^- & Q_B^+ \\ Q_{\tilde{B}}^- & Q_{\tilde{B}}^+ \end{vmatrix} \propto Q_A(u) Q_\theta(u). \quad (2.26)$$

By doing this we will be able to replace  $B$  by  $\tilde{B}$  in (2.19). Let us also show that we can use  $Q_{\tilde{B}}$  instead of  $Q_B$  in the expression for the energy (2.14). We recall that  $Q_\theta(u) \propto u^L$ , so evaluating (2.26) at  $u = 0$  we get

$$Q_B(-\frac{i}{2}) Q_{\tilde{B}}(+\frac{i}{2}) = Q_B(+\frac{i}{2}) Q_{\tilde{B}}(-\frac{i}{2}). \quad (2.27)$$

We can also differentiate (2.26) in  $u$  once and then set  $u = 0$ , so that

$$Q'_B(-\frac{i}{2}) Q_{\tilde{B}}(+\frac{i}{2}) + Q_B(-\frac{i}{2}) Q'_{\tilde{B}}(+\frac{i}{2}) = Q'_B(+\frac{i}{2}) Q_{\tilde{B}}(-\frac{i}{2}) + Q_B(+\frac{i}{2}) Q'_{\tilde{B}}(-\frac{i}{2}). \quad (2.28)$$

Dividing (2.28) by (2.27) we get

$$\frac{Q'_B(-\frac{i}{2})}{Q_B(-\frac{i}{2})} + \frac{Q'_{\tilde{B}}(+\frac{i}{2})}{Q_{\tilde{B}}(+\frac{i}{2})} = \frac{Q'_B(+\frac{i}{2})}{Q_B(+\frac{i}{2})} + \frac{Q'_{\tilde{B}}(-\frac{i}{2})}{Q_{\tilde{B}}(-\frac{i}{2})}, \quad (2.29)$$

which indeed gives

$$E = i\partial_u \log \frac{Q_B^+}{Q_B^-} \Big|_{u=0} = i\partial_u \log \frac{Q_{\tilde{B}}^+}{Q_{\tilde{B}}^-} \Big|_{u=0}. \quad (2.30)$$

**Better notation for  $Q$ -functions** One can combine the above duality transformations and say dualise  $Q_A$  after dualising  $Q_B$  and so on. In order to keep track of all possible transformations one should introduce some notation, as otherwise we can end up with multiple tildas. Another question we will try to answer in this part is how many equivalent BA's we will generate by applying the duality many times to various nodes.

In order to keep track of the dualities we place numbers 1, 2, 3 in between the nodes of the Dynkin diagram. We place the  $Q$ -functions on the nodes of the diagram as in Fig.2.2. Then we interpret the duality as an exchange of the corresponding labels sitting on the links of the diagram, so if before the dualization of  $Q_A$  we had 1, 2, 3, after the duality we have to exchange the indexes 1 and 2 obtaining 2, 1, 3. If instead we first dualised  $Q_B$  we would obtain 1, 3, 2. Each duality produces a permutation of the numbers. We also use these numbers to label the  $Q$ -functions. Namely we assign the indexes to the  $Q$  function in accordance with the numbers appearing above the given node. So, in particular, in the new notation

$$Q_A = Q_1 \quad , \quad Q_B = Q_{12} \quad . \quad (2.31)$$

Each order of the indexes naturally corresponds to a particular set of Bethe equations. For instance, the initial set of Bethe equations on  $Q_A, Q_B$  correspond to the order 1, 2, 3 and the Bethe ansatz (BA) for  $Q_{\bar{A}}, Q_{\bar{B}}$  correspond to 2, 1, 3 and so on. Now we can answer the question of how many dual BA systems we could have; this is given by the number of permutations of 1, 2, 3 i.e. for the case of  $SU(3)$  we get 6 equivalent systems of BA equations.

Following our prescription we also denote

$$Q_{\bar{A}} = Q_2 \quad , \quad Q_{\bar{B}} = Q_{13} \quad . \quad (2.32)$$

We note that we should not distinguish  $Q$ 's which only differ by the order of indexes. So, for instance,  $Q_{21}$  and  $Q_{12}$  is the same  $Q_B$ . We can count the total number of various  $Q$ -functions we could possibly generate with the dualities:  $2^3 - 2 = 6$  different  $Q$ -functions which are

$$Q_i \quad , \quad Q_{[ij]} \quad , \quad i, j = 1, \dots, 3 \quad (2.33)$$

for completeness we also add  $Q_\emptyset \equiv 1$  and  $Q_{123} = Q_{[ijk]} \equiv Q_\theta = u^L$  so that in total we have  $2^3$ . For general  $SU(N)$  we will find  $2^N$  different  $Q$ -functions. We see that the number of the  $Q$ -functions grows rapidly with the rank of the symmetry group. For  $PSU(2, 2|4)$  we get 256 functions, and we should study the relations among them in more detail.

**QQ-relations** Let us rewrite the Bosonic duality in the new notation. The relation (2.23) becomes

$$\left| \begin{array}{cc} Q_i^- & Q_i^+ \\ Q_j^- & Q_j^+ \end{array} \right| \propto Q_{ij} Q_\emptyset \quad (2.34)$$

where we added  $Q_\emptyset = 1$  to the r.h.s. to make both l.h.s and r.h.s be bilinear in  $Q$ . Very similarly (2.26) gives

$$\left| \begin{array}{cc} Q_{12}^- & Q_{12}^+ \\ Q_{13}^- & Q_{13}^+ \end{array} \right| \propto Q_1(u) Q_{123}(u) \quad . \quad (2.35)$$

We see that both identities can be written in one go as

$$\left| \begin{array}{cc} Q_{Ii}^- & Q_{Ii}^+ \\ Q_{Ij}^- & Q_{Ij}^+ \end{array} \right| \propto Q_I(u) Q_{Iij}(u) \quad , \quad (2.36)$$

where for general  $SU(N)$  we would have  $i = 1, \dots, N$  and  $j = 1, \dots, N$  and  $I$  represents a set of indexes such that in (2.35) it is an empty set  $I = \emptyset$  and for the second identity (2.36)  $I$  contains only one element 1. Note that no indexes inside  $I$  are involved with the relations and in the r.h.s. we get indexes  $i$  and  $j$  glued together in the new function. We see that proceeding in this way we can build any  $Q$ -function starting from the basic  $Q_i$  with one index only. For that we can first take  $I = \emptyset$  and build  $Q_{ij}$ , then take  $I = i$  and build  $Q_{ijk}$  and so on. It is possible to combine these steps together to get explicitly

$$Q_{ijk}Q_{\emptyset}^+Q_{\emptyset}^- \propto \begin{vmatrix} Q_i^- & Q_i & Q_i^{++} \\ Q_j^- & Q_j & Q_j^{++} \\ Q_k^- & Q_k & Q_k^{++} \end{vmatrix}. \quad (2.37)$$

Whereas the first identity (2.34) is obvious from the definition, the second (2.37) is a simple exercise to prove from (2.36).

---

**Exercise 11.** Prove (2.37) using the following Mathematica code

```
(*define Q to be absolutely antisymmetric*)
Q[a___] := Signature[{a}] Q @@ Sort[{a}] /; ! OrderedQ[{a}]
(*program bosonic duality*)
Bosonic[J___, i_, j_] := Q[J, i, j][u_] -> (
Q[J, i][u + I/2] Q[J, j][u - I/2] -
Q[J, i][u - I/2] Q[J, j][u + I/2])/Q[J][u];
(*checking the identity*)
Q[1, 2, 3][u] Q[] [u + I/2] Q[] [u - I/2] /. Bosonic[1, 2, 3] /.
Bosonic[1, 2] /. Bosonic[1, 3] /. Bosonic[2, 3] // Factor
```

---

Also derive a similar identity for  $Q_{ijkl}$  using the same code.

---

From the previous exercise it should be clear that we can generate any  $Q_{ij\dots k}$  as a determinant of the basic  $N$   $Q$ -functions  $Q_i$ . In particular the “full-set”  $Q$ -function  $Q_{12\dots N}$ , which is also  $Q_{\theta} = u^L$ , can be written as a determinant of  $N$  basic polynomials  $Q_i$ . Interestingly this identity by itself is constraining enough to give rise to the full spectrum of the  $SU(N)$  spin chain! Indeed  $Q_{12\dots N}$  is a polynomial of degree  $L$  and thus we get  $L$  nontrivial relations on the coefficients of the (twisted) polynomials  $Q_i$ , which together contain exactly  $L$  Bethe roots. This means that this relation alone is equivalent to the whole set of Nested Bethe ansatz equations. So we can put aside a non-unique BA approach, dependent on the choice of the vacuum, and replace it completely by a simple determinant like (2.37). In other words the QQ-relations and the condition of polynomiality is all we need to quantize this quantum integrable model. We will argue that for  $N = 4$  SYM we only have to replace the polynomiality with another slightly more complicated analyticity condition but otherwise keep the same QQ-relations. We will have to, however, understand what the QQ-relations look like for the case of super-symmetries like  $SU(N|M)$ , which is described in the next section.

### 2.3.2 Fermionic duality in $SU(N|M)$

We will see how the discussion in the previous section generalizes to the super-group case. Our starting point will be again the set of nested Bethe ansatz equations, which follow the pattern of the Cartan matrix. Let us discuss the construction of the Bethe ansatz. Below we wrote the Dynkin diagram, Cartan matrix and the Bethe ansatz equations for the  $SU(3|3)$  super spin chain

$$\begin{array}{lcl}
Q_A \circ & \begin{array}{|c|c|c|c|c|} \hline 2 & -1 & 0 & 0 & 0 \\ \hline -1 & 2 & -1 & 0 & 0 \\ \hline 0 & -1 & 0 & +1 & 0 \\ \hline 0 & 0 & +1 & -2 & +1 \\ \hline 0 & 0 & 0 & +1 & -2 \\ \hline \end{array} & \begin{array}{l} -1 = (Q_A^{++}Q_B^-)/(Q_A^{--}Q_B^+) , \quad u = u_{A,i} \\ -1 = (Q_A^-Q_B^{++}Q_C^-)/(Q_A^+Q_B^{--}Q_C^+) , \quad u = u_{B,i} \\ +1 = (Q_B^-Q_D^+)/(Q_B^+Q_D^-) , \quad u = u_{C,i} \\ -1 = (Q_C^+Q_D^{--}Q_E^+)/(Q_C^-Q_D^{++}Q_E^-) , \quad u = u_{D,i} \\ -1 = (Q_D^+Q_E^{--})/(Q_D^-Q_E^{++}) , \quad u = u_{E,i} \end{array}
\end{array} \quad (2.38)$$

The  $Q$ -functions still correspond to the nodes of the Dynkin diagrams and the shift of the argument of the  $Q$ -functions entering the numerators of the Bethe equations simply follow the pattern of the Cartan matrix (with the inverse shifts in numerators). Since the structure of the equations for the bosonic nodes is the same as before, one can still apply the Bosonic duality transformation for instance on  $Q_B$  and replace it by  $Q_{\bar{B}}$ . However for the fermionic type nodes (normally denoted by a crossed circle), such as  $Q_C$ , we get a new type of duality transformation

$$Q_C Q_{\bar{C}} \propto \left| \begin{array}{cc} Q_B^- & Q_B^+ \\ Q_D^- & Q_D^+ \end{array} \right| \quad (2.39)$$

which look similar to the Bosonic one with the difference that we can extract explicitly the dual Baxter polynomial  $Q_{\bar{C}}^4$ . Let us show that the middle Bethe equation can be obtained from the duality relation (2.39). Indeed we see again that for both  $u = u_{C,i}$  and  $u = u_{\bar{C},i}$  we get the middle equation

$$1 = \frac{Q_B^+ Q_D^-}{Q_B^- Q_D^+} , \quad u = u_{\bar{C},i} \quad \text{or} \quad u = u_{C,i}. \quad (2.40)$$

Next we should be able to exclude  $Q_C$  in the other two equations. For that we set  $u = u_{B,i} + i/2$  and  $u = u_{B,i} - i/2$  to get

$$Q_C^+ Q_{\bar{C}}^+ = c(0 - Q_D Q_B^{++}) , \quad Q_C^- Q_{\bar{C}}^- = +c(Q_D Q_B^{--} - 0) \quad u = u_{B,i} . \quad (2.41)$$

Dividing one by the other

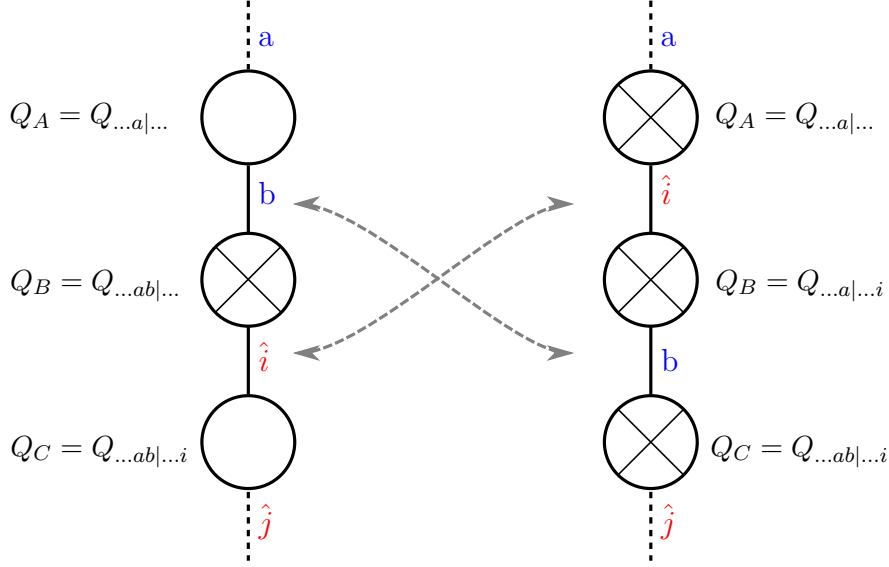
$$-1 = \frac{Q_C^+ Q_{\bar{C}}^+ Q_B^{--}}{Q_C^- Q_{\bar{C}}^- Q_B^{++}} , \quad u = u_{B,i} \quad (2.42)$$

which allows up to exclude  $Q_C$  from the second equation of (2.44). This then becomes

$$-1 = \frac{Q_A^- Q_B^{++} Q_C^-}{Q_A^+ Q_B^{--} Q_C^+} \leftrightarrow +1 = \frac{Q_A^- Q_{\bar{C}}^+}{Q_A^+ Q_{\bar{C}}^-} , \quad u = u_{B,i} . \quad (2.43)$$

<sup>4</sup>Whereas for the Bosonic duality (2.23) the dual Baxter polynomial occur in a complicated way and one had to solve a first order finite difference equation in order to extract it.




**Figure 2.3:** Fermionic duality

As we see this changes the type of the equation from bosonic to fermionic. Thus we also change the type of the Dynkin diagram. This is expected since for super algebras the Dynkin diagram is not unique. Similarly the fourth equation also changes in a similar way. To summarize, after duality we get

$Q_A$	$\bigcirc$	2	-1	0	0	0	$-1 = (Q_A^{++}Q_B^-)/(Q_A^{--}Q_B^+)$	$, u = u_{A,i}$
$Q_B$	$\otimes$	-1	0	+1	0	0	$+1 = (Q_A^- Q_{\tilde{C}}^+)/ (Q_A^+ Q_{\tilde{C}}^-)$	$, u = u_{B,i}$
$Q_{\tilde{C}}$	$\otimes$	0	+1	0	-1	0	$+1 = (Q_B^+ Q_D^-)/ (Q_B^- Q_D^+)$	$, u = u_{\tilde{C},i}$
$Q_D$	$\otimes$	0	0	-1	0	+1	$+1 = (Q_{\tilde{C}}^- Q_E^+)/ (Q_{\tilde{C}}^+ Q_E^-)$	$, u = u_{D,i}$
$Q_E$	$\bigcirc$	0	0	0	+1	-2	$-1 = (Q_D^+ Q_E^{--})/ (Q_D^- Q_E^{++})$	$, u = u_{E,i}$

**Index notation** Again in order to keep track of all possible combinations of dualities we have to introduce index notation. In the super case we label the links in the Dynkin diagram by two types of indexes (with hat and without). The type of the index changes each time we cross a fermionic node. For instance our initial set of Bethe equations corresponds to the indexes  $123\hat{1}\hat{2}\hat{3}$ . The fermionic duality transformation again simply exchanges the labels on the links of the Dynkin diagram (see Fig.2.3). So after duality we get  $12\hat{1}3\hat{2}\hat{3}$ , which is consistent with the  $\bigcirc - \otimes - \otimes - \otimes - \bigcirc$  grading of the resulting Bethe ansatz equations. Finally, we label the  $Q$ -functions by two antisymmetric groups of indexes – with hat and without again simply listing all indexes appearing above the given node of the Dynkin diagram. In particular we get

$$\begin{aligned}
 Q_A &= Q_1 \quad , \quad Q_B = Q_{12} \quad , \quad Q_C = Q_{123} \quad , \\
 Q_{\tilde{C}} &= Q_{12\hat{1}} \quad , \quad Q_D = Q_{123\hat{1}} \quad , \quad Q_E = Q_{123\hat{1}\hat{2}} \quad .
 \end{aligned}
 \tag{2.45}$$

An alternative notation is to omit hats and separate the two sets of indexes by a vertical line:

$$\begin{aligned} Q_A &= Q_{1|\emptyset} \ , \ Q_B = Q_{12|\emptyset} \ , \ Q_C = Q_{123|\emptyset} \ , \\ Q_{\tilde{C}} &= Q_{12|1} \ , \ Q_D = Q_{123|1} \ , \ Q_E = Q_{123|12} \ . \end{aligned} \quad (2.46)$$

---

**Exercise 12.** The fermionic duality transformation changes the type of the Dynkin diagram. The simplest way to understand which diagram one gets after the duality is to follow the indexes attached to the links. Each time the type of the index changes (from hatted to non-hatted) you should draw a cross. List all possible Dynkin diagrams corresponding to  $SU(3|3)$  Lie algebra.

---

**Fermionic QQ-relations** In index notation (2.39) becomes

$$\boxed{Q_{Ib}Q_{I\hat{i}} \propto Q_I^- Q_{I\hat{i}}^+ - Q_I^+ Q_{I\hat{i}}^-} \ . \quad (2.47)$$

For completeness let us write here the bosonic duality relations

$$\boxed{Q_I Q_{Iab} \propto Q_{Ia}^+ Q_{Ib}^- - Q_{Ib}^+ Q_{Ia}^- \ , \ Q_I Q_{I\hat{i}\hat{j}} \propto Q_{I\hat{i}}^+ Q_{I\hat{j}}^- - Q_{I\hat{j}}^+ Q_{I\hat{i}}^-} \ . \quad (2.48)$$

In the case of  $SU(N|M)$  one could derive all  $Q$  functions in terms of  $N + M$  functions  $Q_a$  and  $Q_{\hat{i}}$ . We will demonstrate this in the next section in the example of  $SU(4|4)$ .

## 2.4 QQ-relations for $PSU(2, 2|4)$ Spin Chain

The global symmetry of  $\mathcal{N} = 4$  SYM is  $PSU(2, 2|4)$ . The QQ-relations from the previous section associated with this symmetry constitute an important part of the QSC construction. The symmetry (up to a real form and a projection) is same as  $SU(4|4)$ . In this section we specialize the QQ-relations from the previous part to this case and derive all the most important relations among  $Q$ -functions. In particular we show that all 256 various  $Q$ -functions can be derived from just  $4 + 4$   $Q$ -functions with one index

$$Q_{a|\emptyset} \ , \ Q_{\emptyset|i} \ , \quad (2.49)$$

which are traditionally denoted in the literature as

$$\mathbf{P}_a \ , \ \mathbf{Q}_i \ . \quad (2.50)$$

These are the elementary  $Q$ -functions.

For us, another important object is  $Q_{a|i}$ . According to the general consideration above it can be obtained from the fermionic duality relation (2.47) with  $I = \emptyset$

$$Q_{a|j}^+ - Q_{a|j}^- = \mathbf{P}_a \mathbf{Q}_j \ . \quad (2.51)$$

This is the first order equation on  $Q_{a|i}$  which one should solve; and the formal solution to this equation is<sup>5</sup>

$$Q_{a|j}(u) = - \sum_{n=0}^{\infty} \mathbf{P}_a(u + i\frac{2n+1}{2}) \mathbf{Q}_i(u + i\frac{2n+1}{2}). \quad (2.52)$$

---

**Exercise 13.** Find a solution to the equation (2.51) for  $\mathbf{P}_a \mathbf{Q}_j = e^{\phi u}$  and also for  $\mathbf{P}_a \mathbf{Q}_j = 1/u^2$ .

---

Once we know  $Q_{a|i}$  we can build any  $Q$ -function explicitly in terms of  $Q_{a|i}$ ,  $\mathbf{Q}_i$  and  $\mathbf{P}_a$ . For example using the Bosonic duality we can get

$$Q_{ab|i} = \frac{Q_{a|i}^+ Q_{b|i}^- - Q_{a|i}^- Q_{b|i}^+}{\mathbf{Q}_i}. \quad (2.53)$$

In this way we can build all  $Q$ -functions explicitly in terms of  $Q_{a|i}$ ,  $\mathbf{Q}_i$  and  $\mathbf{P}_a$ . There is a nice simplification taking place for  $Q$ -functions with equal number of indexes:

$$Q_{ab|ij} = \begin{vmatrix} Q_{a|i} & Q_{a|j} \\ Q_{b|i} & Q_{b|j} \end{vmatrix} \quad (2.54)$$

---

**Exercise 14.** Prove (2.54) using the following Mathematica code

---

```
(*define Q to be absolutely antisymmetric*)
Q[a___][b___][u_] := Signature[{a}] Signature[{b}]
Q[Sequence @@ Sort[{a}]] [Sequence @@ Sort[{b}]] [u]
/; ! (OrderedQ[{a}] && OrderedQ[{b}])
(*program bosonic and fermionic dualities*)
B1[J___, a_, b_][K___] := Q[J, a, b][K][u_] :=
(Q[J, a][K][u + I/2] Q[J, b][K][u - I/2] -
Q[J, a][K][u - I/2] Q[J, b][K][u + I/2])/Q[J][K][u];
B2[K___][J___, i_, j_] :=
Q[K][J, i, j][u_] := (Q[K][J, i][u + I/2] Q[K][J, j][u - I/2] -
Q[K][J, i][u - I/2] Q[K][J, j][u + I/2])/Q[K][J][u];
F1[K___, a_][J___, i_][u_] := Q[K, a][J, i][u] :=
(Q[K, a][J, i][u - I] Q[K][J][u - I] +
Q[K, a][J][u - I/2] Q[K][J, i][u - I/2])/Q[K][J][u]
F2[K___, a_][J___, i_][u_] := Q[K, a][J, i][u] :=
(Q[K, a][J, i][u + I] Q[K][J][u + I] -
Q[K, a][J][u + I/2] Q[K][J, i][u + I/2])/Q[K][J][u]
(*deriving the identity*)
Q[a, b][i, j][u] /. B1[a, b][i, j] /. B2[a][i, j] /. B2[b][i, j] /.
Flatten[Table[F1[c][k][u + I], {c, {a, b}}, {k, {i, j}}]] /.
Flatten[Table[F2[c][k][u - I], {c, {a, b}}, {k, {i, j}}]] /.
B2[][i, j] // Simplify
```

---

<sup>5</sup>Note that there is a freedom to add a constant to  $Q_{a|i}$ . This freedom is fixed in the twisted case as we should require that  $Q_{a|j}$  has a “pure” asymptotics at large  $u$  i.e.  $e^{\phi_{ai}u} u^\alpha (1 + A_1/u + A_2/u^2 + \dots)$ .

Also derive a similar identity for  $Q_{abc|ijk}$  using the same code. The general strategy is to use the bosonic duality to decompose  $Q$ 's into  $Q$ -functions with fewer indexes. Then use (2.51) to bring all  $Q_{a|k}(u + in)$  to the same argument  $Q_{a|k}(u)$ . After that the expression should simplify enormously. Also show the following identities to hold

$$Q_{abc|ijkl} = \mathbf{Q}_i Q_{abc|jkl}^+ - \mathbf{Q}_j Q_{abc|kli}^+ + \mathbf{Q}_k Q_{abc|lij}^+ - \mathbf{Q}_l Q_{abc|ijk}^+, \quad (2.55)$$

$$Q_{abcd|ijk} = \mathbf{P}_a Q_{bcd|ijk}^+ - \mathbf{P}_b Q_{cda|ijk}^+ + \mathbf{P}_c Q_{dab|ijk}^+ - \mathbf{P}_d Q_{abc|ijk}^+. \quad (2.56)$$

Also check (2.57) and (2.58) below.

In particular for the  $Q$ -function with all indexes  $Q_{1234|1234}$  (remember that the  $Q$ -function with all indexes played an important role in the XXX spin chain giving the external ‘‘potential’’  $Q_\theta = u^L$ ) we get

$$Q_{1234|1234} = \begin{vmatrix} Q_{1|1} & Q_{1|2} & Q_{1|3} & Q_{1|4} \\ Q_{2|1} & Q_{2|2} & Q_{2|3} & Q_{2|4} \\ Q_{3|1} & Q_{3|2} & Q_{3|3} & Q_{3|4} \\ Q_{4|1} & Q_{4|2} & Q_{4|3} & Q_{4|4} \end{vmatrix}. \quad (2.57)$$

Finally, one can show that

$$Q_{1234|1234}^+ - Q_{1234|1234}^- = \sum_{a,i} \mathbf{Q}_i \mathbf{P}_a Q_{1234\check{a},1234\check{i}}^- \quad (2.58)$$

where the check (inverse hat) denotes an ‘‘index annihilator’’ i.e. for example  $Q_{1234\check{4}|...} = Q_{123|...}$  and  $Q_{1234\check{3}|...} = -Q_{123\check{3}4|...} = -Q_{124|...}$  and so on.

**Hodge duality** The  $SU(4|4)$  Dynkin diagram has an obvious symmetry – we can flip it upside down. At the same time the labeling of the  $Q$ -functions essentially breaks this symmetry as we agreed to list all indexes from above a given node and not below. To fix this we can introduce a Hodge dual set of  $Q$ -functions by defining

$$Q^{a_1 \dots a_n | i_1 \dots i_m} \equiv (-1)^{nm} \epsilon^{a_1 \dots a_n b_1 \dots b_{4-n}} \epsilon^{i_1 \dots i_m j_1 \dots j_{4-m}} Q_{b_1 \dots b_{4-n} | j_1 \dots j_{4-m}} \quad (2.59)$$

with  $b_1 < \dots < b_{4-n}$  and  $j_1 < \dots < j_{4-m}$  so that there is only one term in the r.h.s. One can check that these  $Q$ -functions with upper indexes satisfy the same QQ-relations as the initial  $Q$ -functions<sup>6</sup>.

Finally, we already set  $Q_{\emptyset|\emptyset} = 1$  and considering the symmetry of the system we should also set  $Q_{1234|1234} = Q^{\emptyset|\emptyset} = 1$ . In fact that is indeed the case for  $\mathcal{N} = 4$  SYM whereas for the spin chains we have  $Q_\theta = u^L$  attached to one of the ends of the Dynkin diagram, which breaks the symmetry.

Assuming  $Q_{1234|1234} = 1$  we get some interesting consequences. In particular the l.h.s. of (2.58) vanishes and we get

$$\mathbf{Q}_i \mathbf{P}_a Q^{a|i} = 0. \quad (2.60)$$

<sup>6</sup>in particular (2.59) implies  $Q^{\emptyset|1} = +Q_{1234|234}$  and  $Q^{\emptyset|2} = -Q_{1234|134}$  and so on.

Also we can rewrite (2.55) and (2.56) in our new notation

$$\mathbf{P}^a \equiv Q^{a|\emptyset} = Q^{a|i}(u + i/2)\mathbf{Q}_i, \quad (2.61)$$

$$\mathbf{Q}^i \equiv Q^{\emptyset|i} = Q^{a|i}(u + i/2)\mathbf{P}_a. \quad (2.62)$$

Combining that with (2.60) we get

$$\mathbf{P}_a\mathbf{P}^a = \mathbf{Q}_i\mathbf{Q}^i = 0. \quad (2.63)$$

Finally we can expand the determinant of the  $4 \times 4$  matrix in (2.57) in the first row to get

$$1 = Q_{1|1}Q_{234|234} - Q_{1|2}Q_{234|134} + Q_{1|3}Q_{234|124} - Q_{1|4}Q_{234|123}, \quad (2.64)$$

which is equivalent to  $-1 = Q_{1|a}Q^{1|a}$ . Also we can replace the first row in (2.57) by  $Q_{2|i}$  instead of  $Q_{1|i}$  to get zero determinant. At the same time expanding this determinant in the first row will result in  $0 = Q_{2|a}Q^{1|a}$ . At the end we will get the following general expression

$$Q_{i|a}Q^{j|a} = -\delta_i^j \quad (2.65)$$

which implies that  $Q^{i|a}$  is inverse to  $Q_{i|a}$ .

With these relations, we have completed the task of building the QQ-relations for  $SU(4|4)$  symmetry (with an additional condition that  $Q_{1234|1234} = 1$ , which can be associated with ‘P’ in  $PSU(2, 2|4)$ ). The next step is to understand the analytical properties of the  $Q$ -functions. For the case of the spin chain all  $Q$ -functions are simply polynomials and it was sufficient to produce the spectrum from the QQ-relations. However, in that construction there is no room for a continuous parameter – the ’t Hooft coupling  $g = \frac{\sqrt{\lambda}}{4\pi}$  and thus for the  $N = 4$  SYM the analytical properties should be more complicated and we will motivate the analyticity in the next section. The analytical properties are the missing ingredients in the construction and to deduce them we will have to revise the strong coupling limit.



# Classical String and Strong Coupling Limit of QSC

In this section we briefly describe the action of the super-string in  $AdS^5 \times S^5$ , following closely [1]. We also advice to study the lecture notes of K.Zarembo from the same Les Houches summer school.

## 3.1 Classical String Action

The classical action is similar to the action of the principal chiral field (PCF), so let us briefly review it. The fields  $g(\sigma, \tau)$  in PCF belong to the  $SU(N)$  group. One builds “currents” out of them by

$$J_\mu \equiv -g^{-1} \partial_\mu g \tag{3.1}$$

and then the classical action is simply

$$S = \frac{\sqrt{\lambda}}{4\pi} \int \text{tr}(J \wedge J) . \tag{3.2}$$

The global symmetry of this action is  $SU_L(N) \times SU_R(N)$  since we can change  $g(\sigma, \tau) \rightarrow h_L g(\sigma, \tau) h_R$  for arbitrary  $h_L, h_R \in SU(N)$  without changing the action.

The construction for the Green-Schwartz superstring action is very similar. We take  $g \in SU(2, 2|4)$  and then the current  $J$  (taking values in the  $su(2, 2|4)$  algebra) is built in the same way as in (3.1). The only new ingredient is that we have to decompose the current into 4 components in order to ensure an extra local  $sp(2, 2) \times sp(4)$  symmetry in the way described below.

The superalgebra  $su(2, 2|4)$  can be represented by  $8 \times 8$  supertraceless supermatrices

$$M = \left( \begin{array}{c|c} A & B \\ \hline C & D \end{array} \right) \tag{3.3}$$

where  $A \in u(2, 2)$  and  $B \in u(4)$  and the fermionic components are related by

$$C = B^\dagger \left( \begin{array}{cc} 1_{2 \times 2} & 0 \\ 0 & -1_{2 \times 2} \end{array} \right) . \tag{3.4}$$

An important property of the  $su(2, 2|4)$  superalgebra is that there is a  $Z_4$  automorphism (meaning that one should act 4 times to get a trivial transformation). This  $Z_4$  automorphism has its counterpart in the QSC construction as we discuss later. Its action on an element of the algebra is defined in the following way:

$$\phi[M] \equiv \left( \begin{array}{c|c} EA^T E & -EC^T E \\ \hline EB^T E & ED^T E \end{array} \right) , \quad E = \begin{pmatrix} 0 & -1 & 0 & 0 \\ 1 & 0 & 0 & 0 \\ 0 & 0 & 0 & -1 \\ 0 & 0 & 1 & 0 \end{pmatrix} . \quad (3.5)$$

It is easy to see that  $\phi^4 = 1$ . The consequence of this is that any element of the algebra can be decomposed into the sum  $M = M^{(0)} + M^{(2)} + M^{(3)} + M^{(4)}$ , such that  $\phi[M^{(n)}] = i^n M^{(n)}$ .

---

**Exercise 15.** Find  $M^{(n)}$  for  $n = 0, 1, 2, 3$  explicitly in terms of  $A, B, C, D, E$ .

---

The invariant part  $M^{(0)}$  is exactly  $sp(2, 2) \times sp(4)$ . In particular we can decompose the current  $J = J^{(0)} + J^{(1)} + J^{(2)} + J^{(3)}$  and define the action as

$$S = \frac{\sqrt{\lambda}}{4\pi} \int \text{str} (J^{(2)} \wedge *J^{(2)} - J^{(1)} \wedge J^{(3)}) . \quad (3.6)$$

---

**Exercise 16.** Show that  $M^{(0)} \in sp(2, 2) \times sp(4)$ .

---

**Exercise 17.** The fact that the action does not contain  $J^{(0)}$  guarantees the local invariance of the action w.r.t.  $sp(2, 2) \times sp(4)$ . Explain why.

---

The equations of motion which one can derive from the action (3.6) are

$$\partial_\mu k_\mu = 0 , \quad k_\mu = gK_\mu g^{-1} , \quad K = J^{(2)} + \frac{1}{2} * J^{(1)} - \frac{1}{2} * J^{(3)} . \quad (3.7)$$

One can also interpret  $k_\mu$  as a Noether charge w.r.t to the global  $PSU(2, 2|4)$  symmetry  $g \rightarrow hg$ .

---

**Exercise 18.** Derive  $k_\mu$  from Noether's theorem.

---

## 3.2 Classical Integrability

The equations of motion (3.7) and the flatness condition:

$$dJ - J \wedge J = 0 \quad (3.8)$$

can be packed into the flatness condition of the 1-form

$$A(u) = J^{(0)} + \frac{u}{\sqrt{u^2 - 4g^2}} J^{(2)} - \frac{2g}{\sqrt{u^2 - 4g^2}} * J^{(2)} , \quad u \in \mathbb{C} \quad (3.9)$$

where we use that classically we can set  $J^{(1)} = J^{(3)} = 0$ , as these fermionic parts only become relevant at 1-loop level.



---

**Exercise 19.** By expanding in Taylor series in  $u$  show that each term in the expansion is zero as a consequence of (3.7) and (3.8), i.e.

$$dA(u) - A(u) \wedge A(u) = 0 \quad , \quad \forall u. \quad (3.10)$$

Hint: First verify (3.10) for  $u = 0$ . For that you will have to project the equation (3.8) into  $Z_4$  components first. For example

$$dJ^{(0)} - J^{(0)} \wedge J^{(0)} - J^{(2)} \wedge J^{(2)} = 0. \quad (3.11)$$


---

The existence of the flat connection  $A(u)$ , depending on a spectral parameter  $u$  implies integrability of the model at least at the classical level. Note that (3.10)<sup>1</sup> implies that  $A(u)$  is a “pure gauge” i.e. there exists a matrix valued function  $G(\sigma, \tau, u)$  such that

$$A_\mu(u) = -G^{-1} \partial_\mu G. \quad (3.12)$$

A way to build  $G$  is to compute the Wilson line from some fixed point to  $(\sigma, \tau)$

$$G(\sigma, \tau, u) = \text{Pexp} \int^{(\sigma, \tau)} A(u). \quad (3.13)$$

Using  $G$  we can build the monodromy matrix (which is a super matrix  $(4+4) \times (4+4)$ )

$$\Omega(u, \tau) = G^{-1}(0, \tau, u) G(2\pi, \tau, u) = \text{Pexp} \oint_\gamma A(u). \quad (3.14)$$

where  $\gamma$  is a closed path starting and ending at some point on the worldsheet and wrapping around once. The flatness condition allows us to deform the contour freely provided the endpoints are fixed. Shifting the whole path in time will produce a similarity transformation of  $\Omega(u, \tau)$ .

---

**Exercise 20.** Show that the eigenvalues of  $\Omega(u, \tau)$  do not depend on  $\tau$  if  $A$  is flat.

---

We denote the eigenvalues of  $\Omega(u, \tau)$  as

$$\{e^{ip_1}, e^{ip_2}, e^{ip_3}, e^{ip_4} | e^{ip_{\hat{1}}}, e^{ip_{\hat{2}}}, e^{ip_{\hat{3}}}, e^{ip_{\hat{4}}}\}. \quad (3.15)$$

These functions of the spectral parameter  $u$  are called quasi-momenta. Since they do not depend on time they represent a generating function for conserved quantities. One can, for instance, expand  $p_i(u)$  in the Taylor series at large  $u$  to obtain infinitely many integrals of motion which leads to integrability of string theory. Below we study the analytic properties of the quasimomenta.

---

<sup>1</sup>which in more familiar notations becomes  $F_{\mu\nu} = \partial_\mu A_\nu - \partial_\nu A_\mu + [A_\mu, A_\nu] = 0$ .

**“Zhukovsky” square roots** All the quasimomenta have a square root singularity with the branch points at  $\pm 2g$  (inherited from the definition of  $A$  (3.9)). Note that the analytic continuation under the cut changes the sign of the terms with  $J^{(2)}$  in (3.9) which is in fact equivalent to applying the  $Z_4$  automorphism.

At the same time one can show that

$$C^{-1}\Omega(u)C = \tilde{\Omega}^{-ST}(u) \quad , \quad C = \left( \begin{array}{c|c} E & 0 \\ \hline 0 & E \end{array} \right) \quad (3.16)$$

where  $\tilde{\Omega}(u)$  denotes the analytic continuation of  $\Omega(u)$  under the cut  $[-2g, 2g]$ .

**Exercise 21.** Show that

$$C^{-1}MC = -\phi[M]^{ST} \quad (3.17)$$

where  $ST$  denotes super transpose is defined as  $\left( \begin{array}{c|c} A & B \\ \hline C & D \end{array} \right)^{ST} \equiv \left( \begin{array}{c|c} A^T & C^T \\ \hline -B^T & D^T \end{array} \right)$ .

Use this to show that  $C^{-1}AC = -\tilde{A}^{ST}$  (where tilde denotes analytic continuation under the branch cut  $[-2g, 2g]$ ). Then prove (3.16).

Equation (3.16) implies that the eigenvalues of  $\Omega(u)$  are related to the eigenvalues of  $\tilde{\Omega}(u)$  by inversion and possible permutation. This statement in terms of the quasimomenta (3.15) tells us that the analytic continuation of the quasimomenta i.e.  $\tilde{p}_a(u)$  and  $\tilde{p}_i(u)$  results in the change of sign and possible reshuffling. The exact way they reshuffle can be determined by considering some particular classical solutions and building the quasimomenta explicitly. Some examples can be found in [1]. Since all the classical solutions are related to each other continuously one finds that<sup>2</sup>

$$\tilde{p}_1(u) = -p_2(u) \quad , \quad \tilde{p}_2(u) = -p_1(u) \quad , \quad \tilde{p}_3(u) = -p_4(u) \quad , \quad \tilde{p}_4(u) = -p_3(u) \quad . \quad (3.18)$$

This property will play a crucial role in the QSC construction as we discuss in the next section. One can consider (3.18) as a manifestation of  $Z_4$  symmetry of the action.

**Large  $u$  asymptotics and quantum numbers** Another important property of the quasimomenta is that the quantum numbers of the state can be read off from their values at infinity. To see this notice the following property

$$A = -g^{-1} \left( d + *k \frac{2g}{u} \right) g \quad (3.19)$$

where  $k_\mu$  is the Noether current defined in (3.7). This implies that

$$\Omega = -g^{-1} \left( 1 + \frac{2g}{u} \int_0^{2\pi} d\sigma k_\tau \right) g \quad (3.20)$$

<sup>2</sup>It is also possible to shift the quasimomenta by  $2\pi m$  where  $m$  is integer. This is indeed the case for  $p_i$  for the classical solutions which wind in  $S^5$  and  $m$  gives their winding number. The  $AdS^5$  quasimomenta still satisfy (3.18).

using that the charge  $Q_{\text{Noether}} = 2g \int_0^{2\pi} k_\tau d\sigma$  we immediately get

$$\begin{pmatrix} p_1 \\ p_2 \\ p_3 \\ p_4 \\ p_1 \\ p_2 \\ p_3 \\ p_4 \end{pmatrix} \simeq \frac{1}{2u} \begin{pmatrix} +\Delta - S_1 + S_2 \\ +\Delta + S_1 - S_2 \\ -\Delta - S_1 - S_2 \\ -\Delta + S_1 + S_2 \\ +J_1 + J_2 - J_3 \\ +J_1 - J_2 + J_3 \\ -J_1 + J_2 + J_3 \\ -J_1 - J_2 - J_3 \end{pmatrix}. \quad (3.21)$$

where the r.h.s. comes from the diagonalization of  $Q_{\text{Noether}}/u$  (in the fundamental representation). Here  $J_i$  are integer R-charges (which map to the scalar fields in gauge theory),  $S_1, S_2$  are integer Lorentz charges (corresponding to the covariant derivatives) and  $\Delta$  is the dimension of the state, i.e. its energy. Again we will see the quantum counterpart of this formula when we discuss QSC construction in the next section.

**Action variables and WKB quantization** Another reason the quasimomenta were introduced is because they allow us to define the action variables very easily. For non-trivial solutions the quasimomenta have additional quadratic branch cuts, which come from the diagonalization procedure. The integrals around these cuts give the action variables [30]<sup>3</sup>

$$I_C = \frac{1}{2\pi i} \oint_C p_A(u) du, \quad (3.22)$$

where  $C$  is some branch cut of  $p_A(u)$ . Here  $A$  can take any of 8 values. In the Bohr-Sommerfeld quasi-classical quantization procedure one simply imposes  $I_C \in \mathbb{Z}$  to get the first quantum correction. For example in [1] this property was used to obtain the 1-loop quantum spectrum of the string.

### 3.3 Quasimomenta and the Strong Coupling Limit of QSC

To understand how the quasimomenta we introduced above are related to the  $Q$ -functions from the previous section we are going to first get an insight from the harmonic oscillator. Reconstructing the  $\psi$  from  $p$ , but inverting the relation (2.2) we get

$$\psi(x) = e^{-\frac{m\omega x^2}{2\hbar}} Q(x) = e^{\frac{i}{\hbar} \int^x p(x) dx}. \quad (3.23)$$

Similarly to what we found in (3.22) we also had

$$N = \frac{1}{2\pi i} \frac{i}{\hbar} \oint_C p(x) dx, \quad (3.24)$$

---

<sup>3</sup>this property fixes the choice of the spectral parameter  $u$ , which otherwise can be replaced by any  $f(u)$ .

which allows us to identify  $\frac{ix}{\hbar} \rightarrow u$  so that (3.24) and (3.22) become really identical. Under this identification we can deduce from (3.23)

$$Q_A \simeq \exp\left(\int^u p_A(v)dv\right). \quad (3.25)$$

This naive argument indeed produces the right identification for the strong coupling limit (i.e.  $g \rightarrow \infty$ ) of  $\mathbf{P}_a$  and  $\mathbf{Q}_i$  functions introduced earlier. More precisely we get:

$$\mathbf{P}_a \sim \exp\left(-\int^u p_a(v)dv\right), \quad \mathbf{P}^a \sim \exp\left(+\int^u p_a(v)dv\right) \quad (3.26)$$

$$\mathbf{Q}_i \sim \exp\left(-\int^u p_i(v)dv\right), \quad \mathbf{Q}^i \sim \exp\left(+\int^u p_i(v)dv\right). \quad (3.27)$$

Note that at the leading classical level we do not control the preexponential factors and they may contain some order 1 powers of  $u$ . From that we can immediately draw a number of important consequences:

- We can deduce that large  $u$  asymptotics of  $\mathbf{P}_a$  and  $\mathbf{Q}_i$  from (3.21) are of the form  $u^{Q_{\text{Noether}}/2}$ .
- We can no longer expect that  $\mathbf{P}_a$  or  $\mathbf{Q}_i$  are polynomials as the expressions (3.26) have Zhukovsky branch cuts  $[-2g, 2g]$ .
- From (3.18) we can deduce the following analytic continuation under the branch cut

$$\tilde{\mathbf{Q}}_i \sim \exp\left(+\int^u \tilde{p}_i(v)dv\right) = \exp\left(-\int^u p_{\phi_i}(v)dv\right) \sim \mathbf{Q}^{\phi_i} \quad (3.28)$$

where  $\phi_i$  is determined by (3.18) to be  $\phi_1 = 2$ ,  $\phi_2 = 1$ ,  $\phi_3 = 4$ ,  $\phi_4 = 3$ . So more explicitly we should have the following monodromies

$$\tilde{\mathbf{Q}}_1 = \mathbf{Q}^2, \quad \tilde{\mathbf{Q}}_2 = \mathbf{Q}^1, \quad \tilde{\mathbf{Q}}_3 = \mathbf{Q}^4, \quad \tilde{\mathbf{Q}}_4 = \mathbf{Q}^3. \quad (3.29)$$

These relations remain almost intact at the quantum level. The only improvement one should make is to complex conjugate the r.h.s., as at the quantum level the  $Q_i$  are not real

$$\tilde{\mathbf{Q}}_1 = \bar{\mathbf{Q}}^2, \quad \tilde{\mathbf{Q}}_2 = \bar{\mathbf{Q}}^1, \quad \tilde{\mathbf{Q}}_3 = \bar{\mathbf{Q}}^4, \quad \tilde{\mathbf{Q}}_4 = \bar{\mathbf{Q}}^3. \quad (3.30)$$

The reason for the complex conjugation will become clear in the next Chapter.

To conclude this section we notice that we managed to get all the crucial additional information we have to add to the QQ-relations from just classical limit. Namely, the existence of the Zhukovsky cut and the “gluing” conditions (5.13). In the next chapter we combine all the information together and give the complete description of the spectrum of  $N = 4$  SYM by means of the QSC.

## QSC Formulation

The goal of this section is to summarize the insights we got from the classical limit and from the spin chains and to motivate further the analytic properties of the basic  $\mathbf{P}_a$ ,  $\mathbf{P}^a$ ,  $\mathbf{Q}_i$ ,  $\mathbf{Q}^i$  Q-functions.

### 4.1 Main QQ-Relations

The Q-functions of the  $\mathcal{N} = 4$  SYM satisfy exactly the same QQ-relations as those of the  $SU(4|4)$  spin chain. So we simply summarize the most important relations from Sec.2.4 here to make this section self-contained

$$Q_{a|i}^+ - Q_{a|i}^- = \mathbf{P}_a \mathbf{Q}_i \quad , \quad (4.1)$$

$$\mathbf{P}_a \mathbf{P}^a = \mathbf{Q}_i \mathbf{Q}^i = 0 \quad , \quad (4.2)$$

$$\mathbf{Q}_i = -\mathbf{P}^a Q_{a|i}^+ \quad , \quad (4.3)$$

$$\mathbf{Q}^i = +\mathbf{P}_a Q^{a|i+} \quad , \quad (4.4)$$

$$Q^{a|i} = -(Q_{a|i})^{-t} \quad . \quad (4.5)$$

We also note that the first identity (4.1) can be combined with (4.3) into

$$Q_{a|i}^+ - Q_{a|i}^- = -\mathbf{P}_a \mathbf{P}^b Q_{b|i}^+ \quad . \quad (4.6)$$

This relation tells us that we can use 8 functions  $\mathbf{P}_a$  and  $\mathbf{P}^a$  as the basis to reconstruct all other Q-functions i.e. we can in principle solve (4.6) in terms of  $\mathbf{P}$ 's (we will have an example in the next sections). Then we can use  $Q_{a|i}$  to find  $Q^{a|i}$  as its inverse (4.5). Then one can reconstruct  $\mathbf{Q}_i$  and  $\mathbf{Q}^i$  using (4.3) and (4.4).

The advantage of this choice of basis is, as we explain below, due to the fact that the analytic properties of  $\mathbf{P}_a$  and  $\mathbf{P}^a$  are the simplest among all Q-functions and they can be very efficiently parameterized.

## 4.2 Large $u$ Asymptotic and the Quantum Numbers of the State

The large  $u$  asymptotics of  $\mathbf{P}$ 's and  $\mathbf{Q}$ 's can be deduced from their classical limit (3.26) and (3.21). The main complication here is that in the non-twisted theory there are some additional powers of  $u$  coming from the pre-exponent of (3.26), which modify the asymptotic by  $\pm 1$ . To fix the asymptotic completely one can make comparison with the Asymptotic Bethe Ansatz of Beisert-Staudacher, which can be derived as a limit of QSC. We don't discuss this calculation here but this was done in detail in the original paper [11]. Here we just quote the result

$$\mathbf{P}_a \simeq A_a u^{-\tilde{M}_a}, \quad \mathbf{Q}_i \simeq B_i u^{\hat{M}_i - 1}, \quad \mathbf{P}^a \simeq A^a u^{\tilde{M}_a - 1}, \quad \mathbf{Q}^i \simeq B^i u^{-\hat{M}_i}, \quad (4.7)$$

where

$$\tilde{M}_a = \left\{ \frac{J_1 + J_2 - J_3 + 2}{2}, \frac{J_1 - J_2 + J_3}{2}, \frac{-J_1 + J_2 + J_3 + 2}{2}, \frac{-J_1 - J_2 - J_3}{2} \right\} \quad (4.8)$$

$$\hat{M}_i = \left\{ \frac{\Delta - S_1 - S_2 + 2}{2}, \frac{\Delta + S_1 + S_2}{2}, \frac{-\Delta - S_1 + S_2 + 2}{2}, \frac{-\Delta + S_1 - S_2}{2} \right\} \quad (4.9)$$

we see that indeed the asymptotics are consistent with what we found in the classical limit. Another way to understand the shift by  $\pm 1$  in the asymptotic is to consider a more general twisted theory. The twists (like the parameter  $\phi$  we introduced in the spin chain section) remove many degeneracies<sup>1</sup>. For example without the twist the leading asymptotic in the l.h.s. of (4.1) cancels and one needs to know the subleading term to deduce the asymptotic of the r.h.s. This does not happen in the twisted case when  $Q_{a|i} \sim e^{\phi_{a,i} u} u^{M_{a,i}}$  and the asymptotic behaves more predictably. As a result in the twisted theory there are no  $\pm 1$  shifts w.r.t. the classical limit asymptotic and one can alternatively derive (4.7) by considering first the twisted  $\mathcal{N} = 4$  SYM and then removing them.

**Finding normalization of  $\mathbf{P}$  and  $\mathbf{Q}$**  We will see in the next section that in the near BPS limit  $\mathbf{P}$  and  $\mathbf{Q}$  become small which will allow us to solve the QSC exactly at finite coupling. In order to see this we derive a more general result for the coefficients  $A_a$ ,  $A^a$  and  $B_i$ ,  $B^i$  from (4.7).

---

**Exercise 22.** Use (4.1) and (4.7) to show that

$$Q_{a|j} \simeq -i A_a B_j \frac{u^{-\tilde{M}_a + \hat{M}_j}}{-\tilde{M}_a + \hat{M}_j}. \quad (4.10)$$

---

<sup>1</sup>see [31] for more details about the twisted version of QSC.

From (4.10) we can fix the constants  $A^a$  and  $B^i$  in terms of  $\tilde{M}_a$  and  $\hat{M}_j$ . Substituting the asymptotic (4.10) into (4.3) we get

$$-A^a u^{\tilde{M}_a-1} \left( -i A_a B_j \frac{u^{-\tilde{M}_a+\hat{M}_j}}{-\tilde{M}_a+\hat{M}_j} \right) = B_j u^{\hat{M}_j-1}, \quad (4.11)$$

which simplifies to

$$-1 = i \sum_{a=1}^4 \frac{A^a A_a}{\tilde{M}_a - \hat{M}_j}, \quad (4.12)$$

which allows us to find the combinations  $A^1 A_1$ ,  $A^2 A_2$  and so on. Solving this linear system we find

$$A^{a_0} A_{a_0} = i \frac{\prod_j (\tilde{M}_{a_0} - \hat{M}_j)}{\prod_{b \neq a_0} (\tilde{M}_{a_0} - \tilde{M}_b)}, \quad B^{j_0} B_{j_0} = i \frac{\prod_a (\hat{M}_{j_0} - \tilde{M}_a)}{\prod_{k \neq j_0} (\hat{M}_{j_0} - \hat{M}_k)}, \quad a_0, j_0 = 1 \dots 4 \quad (4.13)$$

(with no summation over  $a_0$  or  $j_0$  in l.h.s.).

---

**Exercise 23.** Derive the relations (4.13).

---

Interestingly the condition that all  $A^{a_0} A_{a_0} = 0$  for all  $a_0$  singles out the BPS states with protected dimension (which works for physical and even non-physical operators like in the BFKL regime).

---

**Exercise 24.** Find all solutions of  $A^{a_0} A_{a_0} = 0$ ,  $\forall a_0$  in terms of  $J_i$ ,  $S_i$  and  $\Delta$ .

---

Next we investigate the cut structure of  $\mathbf{P}_a$  and  $\mathbf{Q}_i$ .

### 4.3 Analytic Structure of Q-functions

In this section we deduce the analytic properties of  $\mathbf{P}_a$  and  $\mathbf{Q}_i$  functions following a maximal simplicity principle, i.e. we assume simplest possible analytical properties which do not contradict the classical limit and the structure of the QQ-system. In Sec.3 from the strong coupling analysis we deduced that  $\mathbf{P}_a$  and  $\mathbf{Q}_i$  should have cuts with branch points at  $\pm 2g$  (to recall  $g = \frac{\sqrt{\lambda}}{4\pi}$  where  $\lambda$  is the 't Hooft coupling). We can assume that  $\mathbf{P}_a$  should have just one single cut  $[-2g, 2g]$ . Note that since  $\mathbf{P}^a$  is related to  $\mathbf{P}_a$  by the symmetry of flipping the Dynkin diagram upside-down it should also have the same analytic properties.

Note that  $\mathbf{Q}_i$  (and  $\mathbf{Q}^i$ ) cannot have the same analytic properties as  $\mathbf{P}$ 's. Indeed, in general  $\Delta$  in the asymptotic of  $\mathbf{Q}_i$  is not-integer and thus we must have a nontrivial monodromy around infinity.<sup>2</sup> The simplest way to gain such a monodromy is to

---

<sup>2</sup>Depending on the values of  $J_i$  there could be a similar issue with  $\mathbf{P}_a$  as the asymptotic could contain half-integer numbers. Strictly speaking  $\mathbf{P}_a$  could have an extra cut going to infinity which would disappear in any bi-linear combinations of  $\mathbf{P}$ s.



**Figure 4.1:** cut structure of  $\mathbf{P}_a$ ,  $\mathbf{P}^a$  and  $\mathbf{Q}_i$ ,  $\mathbf{Q}^i$ .

choose the branch cut to close through infinity i.e. we can assume that  $\mathbf{Q}_i$  and  $\mathbf{Q}^i$  have a “long” branch-cut  $(-\infty, -2g] \cup [+2g, +\infty)$ . This simple argument leads us to the simple analyticity picture Fig.4.1, which historically was derived using the TBA approach in [11].

Note that  $\mathbf{P}$  and  $\mathbf{Q}$  are additionally constrained to be a part of the same Q-system. This makes it very inconvenient to have different conventions for the choice of the branch cuts so we may need to look under the long cut of  $\mathbf{Q}$ . A simple way to explore the space under the cut of  $\mathbf{Q}$  is to use the QQ-relation (4.6) written in the form

$$Q_{a|i}^+ + \mathbf{P}_a \mathbf{P}^b Q_{b|i}^+ = Q_{a|i}^- \quad (4.14)$$

which implies that

$$\begin{aligned} Q_i &= -\mathbf{P}^a Q_{a|i}^+ = -\mathbf{P}^a (\delta_a^b + \mathbf{P}_a^{[+2]} \mathbf{P}^{b[+2]}) Q_{b|i}^{[3]} \\ &= -\mathbf{P}^a (\delta_a^b + \mathbf{P}_a^{[+2]} \mathbf{P}^{b[+2]}) (\delta_b^c + \mathbf{P}_b^{[+4]} \mathbf{P}^{c[+4]}) Q_{c|i}^{[5]} = \dots \end{aligned} \quad (4.15)$$

First we note that from the formal solution (2.52) we can always assume that  $Q_{a|i}$  is regular in the upper half plane. From that we see that (4.15) implies that  $\mathbf{Q}_i$  has an infinite ladder of cuts. The first term in the last line of (4.15) has a cut at  $[-2g, 2g]$ , the second has the cut at  $[-2g - i, 2g - i]$  and so on. See Fig.4.2. The puzzle is how to make this structure of cuts compatible with the initial guess that  $\mathbf{Q}_i$  has only one cut going to infinity. In fact there is no contradiction so far as in order to see the infinite ladder of the cuts we should go to the right from the branch point at  $2g$  i.e. under the long cut. At the same time if we want to go to the lower half plane avoiding the long cut we should go under the first short cut. What is expected to be seen under the first short cut is no branch point singularities below the real axis. Thus if we denote by  $\tilde{\mathbf{Q}}_i$  the analytic continuation of  $\mathbf{Q}_i$  under the first cut it will have no branch cut singularities below the real axis (see Fig.4.2).

From Fig.4.2 we notice an obvious asymmetry of the upper half plane and the lower half plane. Indeed the function  $\mathbf{Q}_i$ , which is a part of Q-system, is analytic in the upper half plane, whereas  $\tilde{\mathbf{Q}}_i$ , which does not necessarily satisfy any QQ-relation is analytic in the lower half plane. I.e. building the Q-system we decided to keep all Q-functions analytic above the real axis and now we potentially lost the symmetry under complex conjugation which can be linked to unitarity of the theory. To reconstruct the symmetry we have to impose the “gluing conditions”.



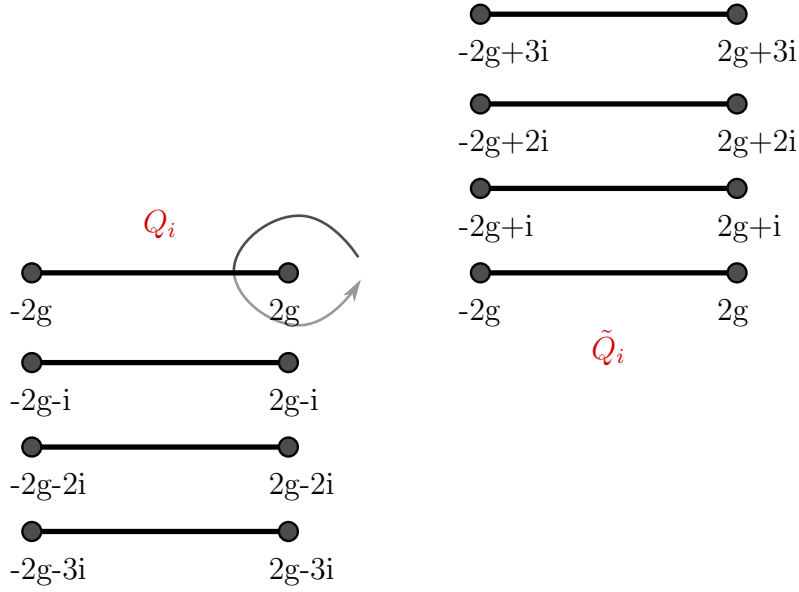


**Figure 4.2:** Analytic structure of  $Q_i$  under its long cut.

## 4.4 Gluing Conditions

In this section we address an imperfection of our construction where the upper half plane plays a more important role from a QQ-relations point of view. To exchange the upper and lower halves we can complex conjugate Q-functions. This procedure does not affect  $\mathbf{P}_a$  and  $\mathbf{P}^a$  much, depending on the normalization constant they can at most change their signs. For  $\mathbf{Q}_i$  the complex conjugation seems to be more dramatic as the ladder of branch cuts going down will now go up. Simply multiplying  $\mathbf{Q}_i$  by a constant would not undo the complex conjugation, however, if we also analytically continue  $\bar{\mathbf{Q}}_i$  under the first branch cut we actually get a very similar analytic structure to the initial  $\mathbf{Q}_i$ ! I.e. the complex conjugation and the analytic continuation should give us back either some  $\mathbf{Q}_i$  or  $\mathbf{Q}^i$ . To determine which of  $\mathbf{Q}$  could do the job we recall that in the classical limit we obtained (5.13) and in accordance with that we impose the following gluing conditions<sup>3</sup>

$$\boxed{\tilde{\mathbf{Q}}_1 \propto \bar{\mathbf{Q}}^2, \quad \tilde{\mathbf{Q}}_2 \propto \bar{\mathbf{Q}}^1, \quad \tilde{\mathbf{Q}}_3 \propto \bar{\mathbf{Q}}^4, \quad \tilde{\mathbf{Q}}_4 \propto \bar{\mathbf{Q}}^3.} \quad (4.16)$$

Together with (4.1)-(4.5), (5.20) constitutes the closed system of QSC equations. It is rather nontrivial that these equations only have a discrete set of solutions (and so far there is no mathematically rigorous proof of this). To demonstrate this we consider some simple examples in the next section and also implement an algorithm which allows us to find solutions numerically.

<sup>3</sup>for physical operators  $\mathbf{Q}_2$  and  $\mathbf{Q}_4$  can mix with  $\mathbf{Q}_1$  and  $\mathbf{Q}_3$  as they are growing faster and have the same non-integer part in the asymptotic (similarly  $\mathbf{Q}^3$  and  $\mathbf{Q}^1$  are defined modulo  $\mathbf{Q}^2$  and  $\mathbf{Q}^4$ ). As a result they are ambiguously defined. Fortunately, we don't have to impose all the 4 of the gluing conditions and it is sufficient to use another pair of equations.

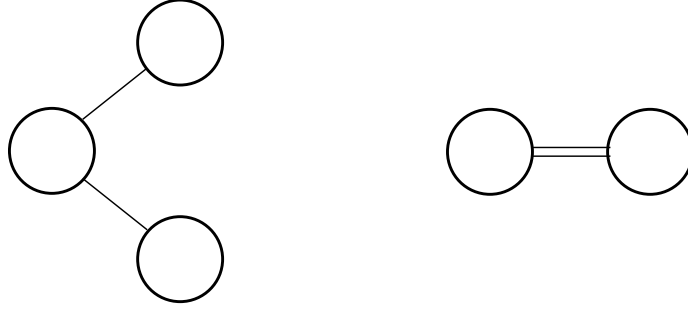


**Figure 4.3:** Under identification of the upper and lower nodes the  $SO(6)$  Dynkin diagram (on the left) becomes the  $SO(5)$  Dynkin diagram (on the right).

## 4.5 Left-Right Symmetric Sub-Sector

In many situations it is sufficient to restrict ourselves to a subset of all states which has an additional symmetry. The left-right (LR) symmetric sub-sector, which includes  $su(2)$  and  $sl(2)$  sub-sectors, contains the states preserving the upside-down symmetry of the Dynkin diagram, i.e. the states which should have  $J_3 = 0$ ,  $S_2 = 0$ . To understand what we should expect in this case consider the bosonic subgroup  $SO(4, 2) \times SO(6)$ . The  $SO(6)$  Dynkin diagram has 3 nodes and imposing the LR symmetry would imply that the nodes 1 and 3 are indistinguishable which reduces the symmetry to  $SO(5)$  (see Fig.4.3). In order to break  $SO(6)$  to  $SO(5)$  it is sufficient to select some preferable direction in the vector 6D representation. Our  $\mathbf{P}_a$  and  $\mathbf{P}^a$  are in 4D fundamental and anti-fundamental representations of  $SO(6)$ . The vector representation can be realized as anti-symmetric tensors with two fundamental indexes  $A_{ab}$  and so we can pick a direction to break  $SO(6)$  to  $SO(5)$  by picking a particular anti-symmetric tensor  $\chi_{ab}$  which can be used to relate fundamental and anti-fundamental representations, i.e. can be used to lower the indexes. In this sub-sector we will get

$$\mathbf{P}_a = \chi_{ab} \mathbf{P}^b . \quad (4.17)$$

Since we have already selected the order of  $\mathbf{P}$ 's by assigning their asymptotic we can see that the only non-zero components of  $\chi$ , consistent with the asymptotic of  $\mathbf{P}$  are 14, 23, 32, 41. Finally we still have freedom to rescale  $\mathbf{P}_a$  to bring  $\chi_{ij}$  to the conventional form

$$\chi_{ab} = \begin{pmatrix} 0 & 0 & 0 & 1 \\ 0 & 0 & -1 & 0 \\ 0 & 1 & 0 & 0 \\ -1 & 0 & 0 & 0 \end{pmatrix} . \quad (4.18)$$

By the same argument we should impose

$$\mathbf{Q}_i = \chi_{ij} \mathbf{Q}^j \quad (4.19)$$

for the same tensor  $\chi_{ij}$ .

## QSC - analytic examples

In this section we consider an example where the QSC can be solved analytically at finite coupling. It is unfortunate that the analytical solutions for physical operators are rather complicated. It is possible to get the solution perturbatively at weak coupling, but this already involves computer algebra. Here instead we consider a non-local operator which can be understood as an analytic continuation of twist- $J$  states. The twist operators are the states with  $J_1 = J$ ,  $J_2 = J_3 = 0$  and  $S_1 = S$ ,  $S_2 = 0$ . They belong to the LR symmetric subsector described in the previous section and below we give the description of the  $sl(2)$  sector to which these states also belong in the next section.

### 5.1 $sl(2)$ Sector

We discuss the simplifications which arise in the  $sl(2)$  sector. As the  $sl(2)$  sector is inside the LR subsector we can restrict ourselves to the Q-functions with lower indexes due to (4.19) and (4.17). The asymptotics of  $\mathbf{P}_a$  (4.7) become

$$\mathbf{P}_1 = A_1 u^{-L/2-1}, \quad \mathbf{P}_2 = A_2 u^{-L/2}, \quad \mathbf{P}_3 = A_3 u^{+L/2-1}, \quad \mathbf{P}_4 = A_4 u^{+L/2}. \quad (5.1)$$

Similarly for  $\mathbf{Q}_i$

$$\begin{aligned} \mathbf{Q}_1 &= B_1 u^{+(\Delta-S)/2}, & \mathbf{Q}_2 &= B_2 u^{+(\Delta+S)/2-1}, \\ \mathbf{Q}_3 &= B_3 u^{-(\Delta+S)/2}, & \mathbf{Q}_4 &= B_4 u^{-(\Delta-S)/2-1}. \end{aligned} \quad (5.2)$$

Also we write (4.13) explicitly for this case

$$\begin{aligned} A_1 A_4 &= -\frac{i(-\Delta + L - S + 2)(-\Delta + L + S)(\Delta + L - S + 2)(\Delta + L + S)}{16L(L + 1)} \\ A_2 A_3 &= -\frac{i(-\Delta + L - S)(-\Delta + L + S - 2)(\Delta + L - S)(\Delta + L + S - 2)}{16(L - 1)L} \end{aligned} \quad (5.3)$$

and

$$\begin{aligned} B_1 B_4 &= -\frac{i(-\Delta + L + S - 2)(-\Delta + L + S)(\Delta + L - S)(\Delta + L - S + 2)}{16\Delta(S - 1)(-\Delta + S - 1)} \\ B_2 B_3 &= +\frac{i(\Delta - L + S - 2)(\Delta - L + S)(\Delta + L + S - 2)(\Delta + L + S)}{16\Delta(S - 1)(\Delta + S - 1)}. \end{aligned} \quad (5.4)$$

We can see that both  $A_a A^a$  and  $B_a B^a$  vanish for  $\Delta \rightarrow L$ ,  $S \rightarrow 0$ . The reason for this is that  $S = 0$  is the BPS protected state and the vanishing of the coefficients indicates the shortening of the multiplet. At the same time when  $\mathbf{P}$  and  $\mathbf{Q}$  are small we get an enormous simplification as we show in the next section where we consider a near BPS limit where  $S$  is small.

## 5.2 Analytic Continuation in $S$

In this section we introduce an analytic continuation in the Lorentz spin  $S_1 = S$ , which for local operators must be integer. The analytic continuation in the spin plays an important role as it links BFKL and DGLAP regimes or high energy scattering in QCD<sup>1</sup>. We leave the questions related to the physics of high energy scattering outside these lectures and describe in detail the analytic continuation in  $S$  from QSC point of view.

The simplest way to describe the analytic continuation is by considering the gluing conditions (5.20), which for LR-symmetric sector reduce to just two

$$\tilde{\mathbf{Q}}_1 \propto \bar{\mathbf{Q}}_3, \quad \tilde{\mathbf{Q}}_2 \propto \bar{\mathbf{Q}}_4, \quad (5.5)$$

since the two others gluing conditions follow by taking complex conjugate and analytically continue the above two conditions.

Also, as we will see that from the numerical analysis in the next section, these two conditions are not independent and only one of them is sufficient to build the spectrum. At the same time imposing both conditions (5.13) leads to the quantization of the charge  $S_1$  whereas keeping only the first condition  $\tilde{\mathbf{Q}}_1 \propto \bar{\mathbf{Q}}_3$  allows us to have  $S_1$  non-integer<sup>2</sup>! However, this will modify the second gluing condition. To constrain the possible form of the modified gluing conditions we denote

$$\tilde{\mathbf{Q}}_i(u) = M_i^j(u) \bar{\mathbf{Q}}_j(u), \quad M_i^j(u) = \begin{pmatrix} 0 & 0 & M_1^3 & 0 \\ M_2^1 & M_2^2 & M_2^3 & M_2^4 \\ M_3^1 & 0 & 0 & 0 \\ M_4^1 & M_4^2 & M_4^3 & M_4^4 \end{pmatrix}_{ij}. \quad (5.6)$$

Since the gluing condition tells us that  $\tilde{\mathbf{Q}}_i$  is essentially the same as  $\mathbf{Q}^i$  up to a possible symmetry of Q-system transformation we should assume that  $M_i^j(u)$  is an  $i$ -periodic function of  $u$ :  $M_i^j(u+i) = M_i^j(u)$ . Furthermore, since  $M_i^j(u)$  relates two functions which are both analytic in the lower half plane it should be analytic.

<sup>1</sup>for the applications of QSC in this regime see [40, 14]

<sup>2</sup>one can show that the second condition necessary leads to the quantization of  $S$  [54]. It could be simpler to check this numerically with the code we explain in the next Chapter.

---

**Exercise 25.** Use periodicity of  $M_i^j$  and equation (5.6) to find  $M_k^j$  explicitly in terms of  $\bar{\mathbf{Q}}_k(u), \bar{\mathbf{Q}}_k(u+i), \bar{\mathbf{Q}}_k(u+2i), \bar{\mathbf{Q}}_k(u+3i)$  and  $\bar{\mathbf{Q}}_j(u), \bar{\mathbf{Q}}_j(u+i), \bar{\mathbf{Q}}_j(u+2i), \bar{\mathbf{Q}}_j(u+3i)$ . From that relation you can see that  $M_k^j$  does not have any branch-cuts, but could possibly have poles. However, existence of poles would contradict the power-like asymptotic of  $\bar{\mathbf{Q}}_j(u)$  and analyticity of  $\tilde{\mathbf{Q}}_i(u)$  as we will have to conclude that  $\bar{\mathbf{Q}}_j$  has infinitely many zeros in the lower half plane, which is impossible with a power-like asymptotic.

---

Armed with the new knowledge of regularity of  $M$  we can analytically continue both sides of (5.6) and complex conjugate them to find the following condition on the matrix  $M$ :

$$\bar{M}(u) = M^{-1}(u) . \quad (5.7)$$

Another constraint comes from the LR-symmetry of the state, which tells us that  $\mathbf{Q}_i = \chi_{ij} \mathbf{Q}^j$ , where  $\mathbf{Q}^j$  is a tri-linear combination of  $\mathbf{Q}_i$  as in (2.37). So using that we get from (5.6)

$$\tilde{\mathbf{Q}}^l(u) = (\chi^{-1})^{li} M_i^j \chi_{jk} \bar{\mathbf{Q}}^k(u) , \quad (5.8)$$

at the same time we can use (2.37) and (2.59) to rewrite the r.h.s. as a combination of 3  $\tilde{\mathbf{Q}}_i$  and then apply the initial (5.6); this results in the following equation

$$\tilde{\mathbf{Q}}^i(u) = -\det(M) (M^{-1})_j^i \bar{\mathbf{Q}}^j(u) . \quad (5.9)$$

Comparing (5.8) and (5.9) we get

$$(\chi^{-1})^{li} M_i^j \chi_{jk} M_n^k = -\det(M) \delta_n^l , \quad (5.10)$$

---

**Exercise 26.** Derive (5.10) by combining (5.8) and (5.9).

---

or in matrix form

$$M \chi M^T = -\chi \det(M) . \quad (5.11)$$

Which implies in particular that  $\det(M) = \pm 1$ . Imposing (5.10) and (5.7) we obtain that  $M$  should reduce to the following form

$$M_i^j(u) = \begin{pmatrix} 0 & 0 & \alpha & 0 \\ \beta & 0 & \gamma & -\bar{\alpha} \\ \frac{1}{\bar{\alpha}} & 0 & 0 & 0 \\ \frac{\gamma}{\alpha\bar{\alpha}} & -\frac{1}{\alpha} & \bar{\beta} & 0 \end{pmatrix}_{ij} , \quad (5.12)$$

with real  $\gamma$ , which results in the following two independent gluing conditions

$$\begin{aligned} \tilde{\mathbf{Q}}_1 &= \alpha \bar{\mathbf{Q}}_3 , \\ \tilde{\mathbf{Q}}_2 &= \beta \bar{\mathbf{Q}}_1 + \gamma \bar{\mathbf{Q}}_3 - \bar{\alpha} \bar{\mathbf{Q}}_4 . \end{aligned} \quad (5.13)$$

Since  $\alpha$  appears both in numerator and denominator it cannot be a non-trivial function of  $u$  as it would create poles. At the same time  $\beta$  and  $\gamma$  can be non-trivial periodic functions of  $u$ . For the case of the twist two operators  $\text{tr} Z D_-^S Z^3$  with non-integer Lorentz spin  $S$  we will verify numerically that  $\gamma$  is a constant and  $\beta = \beta_1 + \beta_2 \cosh(2\pi u) + \beta_3 \sinh(2\pi u)$ . For integer  $S$  both  $\gamma$  and  $\beta$  vanish. Using this gluing matrix one can compute the BFKL pomeron/odderon eigenvalue by analytically continuing to  $S \sim -1$ .

### 5.3 Slope Function

Having the possibility of having the Lorentz spin  $S$  non-integer allows us to study the near-BPS regime  $S \rightarrow 0$  analytically. In this section we will compute the first term linear in  $S$  called to slope function [29] analytically to all orders in  $g$ . This calculation was presented originally in [9] in a slightly different form, there also the next term in small  $S$  expansion was derived. Here we adopt more widely accepted notation of [11], which are different from [9].

The main simplification in this limit is due to the scaling of  $\mathbf{P}_a$  and  $\mathbf{Q}_i$  with  $S \rightarrow 0$  and  $\Delta = L + eS$  where  $e \sim 1$ , which can be deduced from the scaling of  $A_a$  and  $B_i$  (5.3) and (5.4):

$$A_1 A_4 \simeq -B_1 B_4 \simeq -\frac{i}{2}(1-e)S, \quad A_2 A_3 \simeq -B_2 B_3 \simeq -\frac{i}{2}(1+e)S. \quad (5.14)$$

From that we can deduce that  $\mathbf{P}_a$  and  $\mathbf{Q}_i$  both scale as  $\sqrt{S}$ . This assumption in the main simplification – the equation for  $Q_{a|i}$  (4.1) becomes simply

$$Q_{a|i}^+ - Q_{a|i}^- \simeq 0, \quad (5.15)$$

i.e.  $Q_{a|i}$  is a constant! To find which constants they are we can simply use the general formula (4.10) which in our limit gives

$$Q_{a|j} = \begin{pmatrix} -\frac{2iA_1B_1}{(e-1)S} & 0 & 0 & 0 \\ 0 & -\frac{2iA_2B_2}{(e+1)S} & 0 & 0 \\ 0 & 0 & \frac{2iA_3B_3}{(e+1)S} & 0 \\ 0 & 0 & 0 & \frac{2iA_4B_4}{(e-1)S} \end{pmatrix}. \quad (5.16)$$

Using the rescaling symmetry<sup>4</sup> we can set  $B_1 = iA_4$ ,  $B_2 = iA_3$ ,  $B_3 = iA_2$ ,  $B_4 = iA_1$  giving

$$Q_{a|j} = \begin{pmatrix} i & 0 & 0 & 0 \\ 0 & -i & 0 & 0 \\ 0 & 0 & i & 0 \\ 0 & 0 & 0 & -i \end{pmatrix}. \quad (5.17)$$

<sup>3</sup> $Z$  is a complex scalar of the theory,  $D_-$  is a light-cone covariant derivative.

<sup>4</sup>We can rescale  $\mathbf{P}_1 \rightarrow f\mathbf{P}_1$  and  $\mathbf{P}_2 \rightarrow g\mathbf{P}_2$ , rescaling simultaneously  $\mathbf{P}_3 \rightarrow 1/f\mathbf{P}_1$  and  $\mathbf{P}_4 \rightarrow 1/g\mathbf{P}_4$  and similar for  $\mathbf{Q}_i$ . In addition for  $\mathbf{P}$ 's only we have the freedom  $\mathbf{P}_3 \rightarrow \mathbf{P}_3 + \gamma_2\mathbf{P}_2 - \gamma_1\mathbf{P}_1$  and  $\mathbf{P}_4 \rightarrow \mathbf{P}_4 + \gamma_3\mathbf{P}_1 + \gamma_1\mathbf{P}_2$  for some constants  $\gamma_n$ , this ambiguity is resolved in the twisted theory. These transformations are the most general which preserve  $\chi_{ij}$  tensor and do not modify the asymptotic of  $\mathbf{P}$ 's.

This implies that  $\mathbf{Q}_i$  and  $\mathbf{P}_a$  are essentially equal in this limit due to (4.4):

$$\mathbf{Q}_1 = i\mathbf{P}_4 \ , \ \mathbf{Q}_2 = i\mathbf{P}_3 \ , \ \mathbf{Q}_3 = i\mathbf{P}_2 \ , \ \mathbf{Q}_4 = i\mathbf{P}_1 \ . \quad (5.18)$$

This makes our calculations much easier as we can write the gluing condition (5.13) directly on  $\mathbf{P}$

$$\tilde{\mathbf{P}}_4 = -\alpha\bar{\mathbf{P}}_2 \quad (5.19)$$

$$\tilde{\mathbf{P}}_3 - \bar{\alpha}\bar{\mathbf{P}}_1 = -[\beta_1 + \beta_2 \cosh(2\pi u) - \beta_3 \sinh(2\pi u)]\bar{\mathbf{P}}_4 - \gamma\bar{\mathbf{P}}_2 \ . \quad (5.20)$$

To solve these equations we have to impose the asymptotic on  $\mathbf{P}_a$ . For simplicity we consider the  $L = 2$  case only, leaving general  $L$  as an exercise. For  $L = 2$  (5.1) gives:

$$\mathbf{P}_1 \simeq A_1 \frac{1}{u^2} \ , \ \mathbf{P}_2 \simeq A_2 \frac{1}{u} \ , \ \mathbf{P}_3 \simeq A_3 \ , \ \mathbf{P}_4 \simeq A_4 u \ . \quad (5.21)$$

Since  $\mathbf{P}_a$  is a function with only one branch cut which can be resolved with the help of the Zhukovsky variable  $x(u) = \frac{u + \sqrt{u^2 - 4g^2}}{2g}$  we can use the following general ansatz<sup>5</sup>

$$\mathbf{P}_1 = \sum_{n=2}^{\infty} \frac{c_{1,n}}{x^n} \ , \ \mathbf{P}_2 = \sum_{n=1}^{\infty} \frac{c_{2,n}}{x^n} \ , \ \mathbf{P}_3 = \sum_{n=0}^{\infty} \frac{c_{3,n}}{x^n} \ , \ \mathbf{P}_4 = \sum_{n=-1}^{\infty} \frac{c_{4,n}}{x^n} \ . \quad (5.22)$$

Note that under analytic continuation  $\tilde{x} = 1/x$ . Now we can use the condition (5.19) to deduce  $\mathbf{P}_4$  and  $\mathbf{P}_1$ . Plugging the ansatz (5.22) into (5.19) we get

$$\frac{c_{4,-1}}{x} + c_{4,0} + c_{4,1}x + c_{4,2}x^2 + \dots = -\alpha \left( \frac{\bar{c}_{2,1}}{x} + \frac{\bar{c}_{2,2}}{x^2} + \frac{\bar{c}_{2,3}}{x^3} + \dots \right) \ . \quad (5.23)$$

We see that the l.h.s. contains infinitely many positive powers of  $x$  whereas in the r.h.s. there are only negative powers, which implies that  $c_{4,n \geq 0} = 0$  and  $c_{2,n \geq 2} = 0$  and thus

$$\mathbf{P}_2 = \frac{c_{2,1}}{x} \ , \ \mathbf{P}_4 = -\alpha\bar{c}_{2,1}x \ . \quad (5.24)$$

In order to deal with the second equation in a similar way we should use the identities

$$\cosh(2\pi u) = \sum_{n=-\infty}^{\infty} I_{2n}(\sqrt{\lambda}) x^{2n}(u) \ , \ \sinh(2\pi u) = \sum_{n=-\infty}^{\infty} I_{2n+1}(\sqrt{\lambda}) x^{2n+1}(u) \quad (5.25)$$

where  $I_n(z)$  is the Bessel function of 2nd kind defined as

$$I_n(y) = \oint \frac{e^{y/2(z+1/z)} dz}{z^{1-n} 2\pi i} \ . \quad (5.26)$$

---

<sup>5</sup>which can be interpreted as a Laurent series expansion in  $x$  plane, where the functions  $\mathbf{P}$  are analytic in the exterior of the unit circle and the first singularity lies inside the unit circle ensuring good convergence of the series expansion.

---

**Exercise 27.** Prove identities (5.25), you will have to use that  $u = g(x + 1/x)$  and that  $g = \frac{\sqrt{\lambda}}{4\pi}$ .

---

After that we can express both sides of (5.20) as a power series in  $x$  and match the coefficients. In particular comparing the coefficients of  $x^0$  and  $x^{-2}$  we get

$$c_{3,0} = -\alpha\beta_3 c_{2,1} I_1(\sqrt{\lambda}) \quad , \quad c_{1,2} = \frac{\bar{\alpha}\bar{\beta}_3 \bar{c}_{2,1}}{\alpha} I_3(\sqrt{\lambda}) \quad . \quad (5.27)$$

Finally, forming the combinations

$$A_1 A_4 = g c_{4,-1} c_{1,2} = -g \bar{\alpha} \bar{\beta}_3 \bar{c}_{2,1}^2 I_3(\sqrt{\lambda}) \quad (5.28)$$

$$A_2 A_3 = g c_{2,1} c_{3,0} = -g \alpha \beta_3 c_{2,1}^2 I_1(\sqrt{\lambda}) \quad (5.29)$$

which are also given in (5.14) in terms of a real quantity  $e = (\Delta - L)/S$  and  $S$  we conclude that

$$\Delta - L = S \frac{I_1(\sqrt{\lambda}) + I_3(\sqrt{\lambda})}{I_1(\sqrt{\lambda}) - I_3(\sqrt{\lambda})} \quad . \quad (5.30)$$

reproducing the result from [29]!

---

**Exercise 28.** Repeat the above calculation for arbitrary  $L$ . You have to obtain

$$\Delta - L = S \frac{\sqrt{\lambda} I_{L+1}(\sqrt{\lambda})}{L I_L(\sqrt{\lambda})} \quad . \quad (5.31)$$

In the derivation you can assume that  $\gamma = \beta_1 = \beta_2 = 0$ . We explain below why that is the case for  $L = 2$ .

---

In order to fix the solution for  $\mathbf{P}_a$  we notice that we also get

$$c_{2,1}^2 = \frac{iS}{g\alpha\beta_3(I_1(\sqrt{\lambda}) - I_3(\sqrt{\lambda}))} \quad . \quad (5.32)$$

Even though the constants  $\gamma, \beta_1$  and  $\beta_2$  did not enter into the calculation, leading to the dimension  $\Delta$ , they will still appear in the solution for  $\mathbf{P}_a$ . Here we will fix them further from the reality conditions. Let us also show that  $\gamma = \beta_2 = 0$ . First the coefficients  $x$  and  $1/x$  from (5.20) give the following combination

$$\beta_1 = -\beta_2 I_0(\sqrt{\lambda}) \quad , \quad \gamma = -\alpha \beta_2 \frac{c_{2,1}}{\bar{c}_{2,1}} I_2(\sqrt{\lambda}) \quad . \quad (5.33)$$

Since  $c_{2,1}$  is already fixed (5.32) we obtain

$$\frac{\gamma^2 |\beta_3|^2}{|\alpha|^2 I_2^2(\sqrt{\lambda})} = -\beta_2^2 \bar{\beta}_3^2 \quad (5.34)$$



where the l.h.s. is real and positive. At the same time if we compare the coefficients of  $x^2$  and  $x^3$  in (5.20) we get

$$\frac{c_{3,3} I_1(\sqrt{\lambda})}{c_{3,2} I_2(\sqrt{\lambda})} = \frac{\beta_2}{\beta_3} = \frac{\bar{\beta}_2}{\bar{\beta}_3} \quad (5.35)$$

where again the l.h.s. should be real due to the complex conjugation property of  $\mathbf{P}_a$  which allows us to complex conjugate the r.h.s.<sup>6</sup>. Squaring both sides of (5.35) and multiplying by (5.36) we obtain

$$\frac{\gamma^2 |\beta_3|^2}{|\alpha|^2 I_2^2(\sqrt{\lambda})} = -\beta_2^2 \bar{\beta}_2^2, \quad (5.36)$$

which is only possible if  $\beta_2 = \gamma = 0$ .

---

<sup>6</sup>Under the complex conjugation  $\mathbf{P}_a \rightarrow e^{i\phi_a} \mathbf{P}_a$ , for some real  $\phi_a$ . This implies that the ratios  $c_{a,n}/c_{a,m}$  are real.



# Solving QSC at finite coupling Numerically

## 6.1 Description of the Method

In this part of the notes we describe the numerical algorithm and analyze some of the numerical results. We illustrate the general method initially proposed in [13] by considering the same states as in the previous section  $\text{tr} Z D^S Z$  i.e. twist-2 operators. First we consider  $S = 2$  case – Konishi operator. Additionally from the beginning we impose the parity symmetry which this states have i.e. symmetry under  $u \rightarrow -u$  which reflects in the parity of  $\mathbf{P}_a$  functions. The *Mathematica* code which we used for this lecture can be found as an ancillary file for the arXiv submission 1504.06640.

Below we describe the main steps and ideas for the numerical procedure.

- Parameterise the system in terms of the truncated series in  $x$  of  $\mathbf{P}_a$  as follows:

$$\mathbf{P}_a = (xg)^{-\tilde{M}_a} \mathbf{p}_a, \quad \mathbf{p}_a = \left( A_a + \sum_{n=1}^{\infty} \frac{c_{a,n}}{x^{2n}} \right) \quad (6.1)$$

where in the code we cut the sum at some finite value `Pcut`. We will see that to get 6 digits of precision with need `Pcut` as small as 3 (for relatively small  $g = 1/5$ ). This series converges very well even for  $|x| = 1$ . Note that under the analytic continuation to the next sheet we simply replace  $x \rightarrow 1/x$  so that

$$\tilde{\mathbf{P}}_a = (x/g)^{\tilde{M}_a} \left( A_a + \sum_{n=1}^{\infty} c_{a,n} x^{2n} \right). \quad (6.2)$$

- Given  $\mathbf{P}_a$  in terms of  $c_{a,n}$  find  $Q_{a|i}(u)$  as a series expansion in large  $u$ :

$$Q_{a|i}(u) = u^{-\tilde{M}_a + \hat{M}_j} \sum_{n=0}^{\infty} \frac{B_{a,i,n}}{u^{2n}}. \quad (6.3)$$

We find the coefficients  $B_{a,i,n}$  by plugging the expansion (6.3) into the finite difference equation (4.6). The term  $B_{a,i,0}$  we found before in (4.10). Expanding

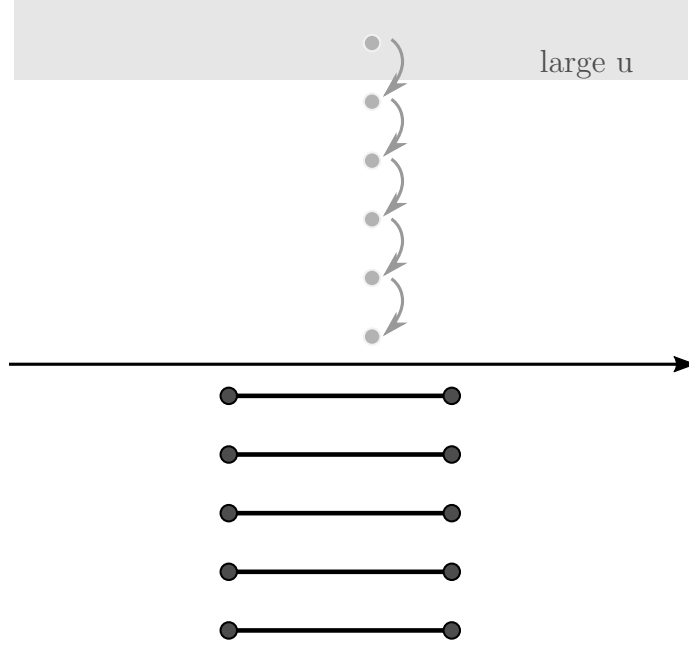


**Figure 6.1:** To reconstruct  $Q_{a|i}$  at the values of  $u \sim 1$  we perform several jumps by  $i$  using (6.4) into the region on the upper half plane where the asymptotic expansion (6.3) is applicable.

it at large  $u$  we get a linear system on the coefficients  $B_{a,i,n}$ . The series (6.3) is asymptotic and works well as far as  $u$  is large enough. In our numerical implementation we keep around 12 terms.

- Starting from the expansion (6.3) at large  $\text{Im}u$  we can move down to the real axis using (4.6) in the form

$$Q_{a|i}(u - \frac{i}{2}) = (\delta_a^b - \mathbf{P}_a(u)\mathbf{P}_c(u)\chi^{cb}) Q_{b|i}(u + \frac{i}{2}). \quad (6.4)$$

Applying (6.4) recursively we can decrease the imaginary part of  $u$  from the asymptotic area to reach finite values of  $u$  (see Fig.6.1). We will mostly need values of  $Q_{a|i}$  at  $\text{Im} u = 1/2$  with  $-2g < \text{Re} u < 2g$ .

- Having  $Q_{a|i}$  computed we reconstruct  $\mathbf{Q}_i$  and  $\tilde{\mathbf{Q}}_i$  from

$$\mathbf{Q}_i(u) = Q_{a|i}(u + i/2)\chi^{ab}\mathbf{P}_b(u) \quad , \quad \tilde{\mathbf{Q}}_i(u) = Q_{a|i}(u + i/2)\chi^{ab}\tilde{\mathbf{P}}_b(u) \quad (6.5)$$

where  $\mathbf{P}_a$  and  $\tilde{\mathbf{P}}_a$  are given in terms of  $c_{a,n}$  in (6.1) and (6.2).

- Finally, we constrain  $c_{a,n}$  from the gluing conditions (5.13). We will see that it is sufficient to impose only half of them. In our numerical implementation we build a function

$$F(\Delta, c_{a,n}, u) = \tilde{\mathbf{Q}}_3 - \alpha\bar{\mathbf{Q}}_1 \quad (6.6)$$

and then adjust  $\Delta$  and  $c_{a,n}$  to minimize  $F(\Delta, c_{a,n}, u)$  at some set of probe points  $u_k \in (2g, 2g)$ . For this we use standard numerical optimization methods.

In the next section we give more details about the *Mathematica* implementation of our method.

## 6.2 Implementation in *Mathematica*

The *Mathematica* notebook we describe below, with slight improvements, can be downloaded from arXiv [13].

First we make basic definitions. We define  $x(u)$  in the way to ensure that it has only one cut  $[-2g, 2g]$

---

```
X[u_] = (u + g*Sqrt[u/g - 2]*Sqrt[u/g + 2])/(2*g);
chi = {{0, 0, 0, -1}, {0, 0, 1, 0}, {0, -1, 0, 0},
{1, 0, 0, 0}};
```

---

**Exercise 29.** What is the branch cut structure of the naive definition

$X[u_]=\frac{(u+\text{Sqrt}[u^2-4g^2])}{(2g)}$  consider also the case of complex  $g$ .

---

Next we define  $\hat{M}$  and  $\tilde{M}$  as in (4.8). We also specialize to the Konishi operator in the  $sl(2)$  sector with  $J_1 = S = 2$ . The variable  $d$  denotes the full dimension  $\Delta$ ;

---

```
J1 = 2; J2 = 0; J3 = 0; S1 = 2; S2 = 0;
Mt = {(J1+J2-J3+2)/2, (J1-J2+J3)/2, (-J1+J2+J3+2)/2, (-J1-J2-J3)/2}
Mh = {(d-S1-S2+2)/2, (d+S1+S2)/2, (-d-S1+S2+2)/2, (-d+S1-S2)/2}
powp = -Mt;
powq = Mh - 1;
(*setting the value for the coupling*)
g = 1/5;
```

---

The variables `powp` and `powq` give the powers of  $\mathbf{P}_a$  and  $\mathbf{Q}_i$ . We also set the coupling to a particular value  $g = 1/5$ .

**Parameters** There are several parameters which are responsible for the precision of the result.

---

```
cutP = 3; (* number of terms we keep in the expansion of P_a *)
cutQai = 12; (* number of powers in expansion of Qai at large *)
shiftQai = 20; (* Number of jumps from asymptotic region *)
WP = 50; (* Working precision *)
P0 = 12; (* Number of the sampling points on the cut to use *)
```

---

**Ansatz for  $\mathbf{P}_a$  and parameters of the problem** The set of  $\mathbf{p}_a$  from (6.1) we define as follows

---

```
ps = {A[1] + I*Sum[c[1, n]/x^(2*n), {n, cutP}],
      A[2] + I*Sum[c[2, n]/x^(2*n), {n, cutP}],
      A[3] + Sum[c[3, n]/x^(2*n), {n, cutP}],
      A[4] + Sum[c[4, n - 1]/x^(2*n), {n, 2, cutP + 1}]};
```

---

Note that we set the first sub-leading coefficient in  $\mathbf{P}_4$  to zero, this is always possible to do due to the residual symmetry (see footnote 4). Whereas the coefficients  $c_{a,n}$  will serve as parameters in the optimization problem, the leading coefficients  $A_a$  are fixed in terms of the quantum numbers of the state via (5.3)

---

```
A[1]=-I Product[(Mt[[1]]-Mh[[j]])/If[j==1,1,Mt[[1]]-Mt[[j]]],{j,4}]
A[2]=+I Product[(Mt[[2]]-Mh[[j]])/If[j==2,1,Mt[[2]]-Mt[[j]]],{j,4}]
A[3] = 1; A[4] = 1;
```

---

Similarly we code the leading coefficients of  $Q_i$  and  $Q_{a|i}$

---

```
B[1]=-I Product[(Mh[[1]]-Mt[[j]])/If[j==1,1,Mh[[1]]-Mh[[j]]],{j,4}]
B[2]=+I Product[(Mh[[2]]-Mt[[j]])/If[j==2,1,Mh[[2]]-Mh[[j]]],{j,4}]
B[3] = 1; B[4] = 1;
(* leading order coefficients in Q_ai *)
Do[B[a,i,0] = -I(A[a]B[i])/(powq[[i]]+powp[[a]]+1),{a,4},{i,4}]
```

---

The whole Q-system, which we are partially going to reconstruct, is thus parameterized by a set of  $c_{i,n}$  and  $d$ . The substitute `sb` will replace these variables by their values stored in the list `params`

---

```
prm := {d}~Join~Flatten[Table[c[i, n], {i, 4}, {n, cutP}]];
sb := Rule @@@ (Transpose[{prm, SetPrecision[params, WP]}])
```

---

We will update the list `params` at each iteration with its better approximation. As we are going to solve it with a Newton-like method, which is very sensitive to the starting points, one should roughly know where to look for the solution. A perturbative solution, available in some cases, could be good to start with, but sometimes even a very rough estimate of  $d$  and a few first coefficients will lead to a convergent procedure. For `cutP=3` we need in total  $1 + 4 * 3 = 13$  parameters.

**Finding  $Q_{a|i}$  at large  $u$**  Having finished with defining the basics we can finally accomplish the first step in the algorithm – find the large  $u$  expansion of  $Q_{a|i}$  in the form (6.3). First we re-expand  $\mathbf{P}_a$  at large  $u$ :

---

```
psu = Series[(g x/u)^powp ps/.x->X[u],{u,Infinity,cutQai+2}];
```

---

Next we define separately the non-integer power  $u^{-\tilde{M}_a+\tilde{M}_j}$  and the series in inverse negative powers (6.3)

---

```
qaipow = Table[u^powq[[i]]*u^powp[[a]]*u, {a, 4}, {i, 4}];
Bpart = Table[Sum[B[a,i,n]/u^(2*n),{n,0,cutQai/2}],{a,4},{i,4}];
```

---

For optimization purposes we pre-expand these parts of the expansion separately with shifts  $u \rightarrow u \pm i/2$

---

```
powP=Series[(qaipow/.u->u+I/2)/qaipow/.(u+a_)^(b_-):>u^b*(1+a/u)^b,
  {u,Infinity,cutQai+2}];
powM=Series[(qaipow/.u->u-I/2)/qaipow/.(u+a_)^(b_-):>u^b*(1+a/u)^b,
  {u,Infinity,cutQai+2}];
BpartP = Series[Bpart /. u -> u + I/2, {u,Infinity,cutQai+2}];
```

---

---

```
BpartM = Series[Bpart /. u -> u - I/2, {u, Infinity, cutQai + 2}];
```

---

Finally we code the function which computes the coefficients  $B_{a,i,n}$

---

```
FindQlarge := Block[{},
PP=Series[KroneckerProduct[psu, chi.psu], {u, Infinity, cutQai+2}]/.sb;
eqs=ExpandAll[Series[Normal[
(BpartP/.sb)*powP-(BpartM/.sb)*powM+(1/u)*PP.(BpartP*powP) /. sb]
,{u, Infinity, cutQai+2}]];
slB = Last[Solve[LogicalExpand[eqs == 0]]];
Qailarge = qaipow*Bpart/.slB/.sb]
```

---

The function computes the expansion and store it in the variable `Qailarge`.

**Finding  $Q_{a_i}$ ,  $Q_i$  and  $\tilde{Q}_i$  on the real axis** In order to impose the gluing conditions on the Zhukovsky branch cut (5.13) we will use a set of sampling points (points), chosen so that their density increases near the ends of the interval  $[-2g, 2g]$  to guarantee maximal efficiency (we use Chebyshev nodes).

---

```
points = N[Table[-2*g*Cos[Pi*((n - 1/2)/PO)], {n, PO}], WP];
```

---

Now for each of the sampling points we have to climb up to the asymptotic region using (6.4).

---

```
SolveQPP[n0_] := Block[{}, Clear[Qai, PP, PS];
PS[uu_] := PS[uu] = SetPrecision[Expand[(x*g)^powp*ps/.sb]
/.x^(a_.)->X[uu]^a /. sb, WP];
PP[(uu_)?NumericQ] := PP[uu] = IdentityMatrix[4]+
KroneckerProduct[PS[uu], chi.PS[uu]];
Qai[n0][uu_] = Qailarge /. u -> uu + I*n0 - I/2;
Qai[n_][u_] := Qai[n][u] = SetPrecision[PP[u+I*n].Qai[n+1][u], WP];
Qaiplist = Table[Qai[1][p], {p, points}];
```

---

This function creates `Qaiplist` which contains values of  $Q_{a_i}$  at the sampling points. This allows us to compute  $Q_i$  using simple matrix multiplication via (6.5)

---

```
DoQlist := Block[{},
Qilist = Transpose[Table[((x*g)^powp*ps/.x->X[u]/.sb
/.u->points[[i]]).chi .Qaiplist[[i]], {i, PO}]];
Qitlist = Transpose[Table[((x*g)^powp*ps/.x->1/X[u]/.sb
/.u->points[[i]]).chi.Qaiplist[[i]], {i, PO}]];];
```

---

Now when we have the values of  $Q_i$  and also  $\tilde{Q}_i$  we can define the function  $F$ , which depends on the parameters  $d, c_{a,n}$  and computes the mismatch of the gluing condition at the sampling points.

---

```
F[Plist_List] := (F[Plist] = Block[{}, Print[Plist];
params = Plist;
FindQlarge;
SolveQPP[shiftQai];
DoQlist;
```

```

C1list = Qilist[[1]]/Conjugate[Qilist[[3]]];
C2list = Qitlist[[1]]/Conjugate[Qitlist[[3]]];
c = Mean[Join[C1list, C2list]];
Flatten[{Re[{C1list-c, C2list-c}/c], Im[{C1list-c, C2list-c}/c]}]]
)/; NumericQ[Total[Plist]];

```

---

Finally, we have to tune the values of parameters so that the square of the function  $F$  is minimized.

---

```

(*setting the starting configuration*)
params0 = SetPrecision[{4.5,0,0,0,-1,0,0,1,0,0,0,0,0}, WP];
(*finding optimal parameters*)
FindMinimum[(1/2)*F[prm].F[prm],
  Transpose[{prm, params0}],
  Method -> {"LevenbergMarquardt", "Residual" -> F[prm]},
  WorkingPrecision -> 30,
  AccuracyGoal -> 7]

```

---

The built-in function `FindMinimum` is rather slow and takes around 10min to run. It is much better to use the implementation from the notebook attached to the arXiv submission [13] which uses parallel computing and gives the result in about 1 minute. It is possible to further improve the above basic code performance by roughly a factor of 10 – 100, but that will also make it more cumbersome.

---

**Exercise 30.** Use the above code to get the dimension of the Konishi operator at  $g = 1/5$ . Compare your result with the high precision evaluation  $\Delta = 4.4188598808023509$  taken from [13].

---

**Exercise 31.** Use the result for  $g = 1/5$  as a starting point to compute  $g = 3/10$ . You should get  $\Delta = 4.826949$ . Note that the convergence radius of the perturbation theory is  $g^* = 1/4^1$ , so this value is already outside the range accessible with perturbation theory.

---

**Exercise 32.** Check that the same code will work perfectly for non-integer values of the Lorentz spin  $S$ . Analytic continuation in the spin is very important for the BFKL applications [40, 14]. Try to change  $S = S_1$  gradually until it reaches  $S = 3/2$  for  $\Delta = 2/10$ . You should get  $\Delta = 3.85815$ . Verify numerically (5.13) and show that  $\gamma \simeq 0.0030371$  is indeed a real constant and  $\beta = \beta_1 + \beta_2 \cosh(2\pi u) + \beta_3 \sinh(2\pi u)$  for some constants  $\beta_k$ .

---

<sup>1</sup>The finite convergence radius of the perturbation theory is due to the branch-cut singularity of the spectrum at  $g_* = \pm i/4$ . This is the value of the coupling when branch points of the Zhukovsky cuts  $2g + in$  and  $-2g + in \pm i$  become equal.



# Applications, Further Reading and Open Questions

In this section we attempt to cover most of the recent applications of the QSC methods and offer some open questions.

**QSC for ABJ(M) Theory** The QSC was also developed for ABJ(M) theory (which is a 3D  $\mathcal{N} = 6$  Chern-Simons theory) in [10, 17]. A nontrivial specific feature of this theory is that the positions of the branch points are related to the 't Hooft coupling in a very nontrivial way and is called the interpolation function  $h(\lambda)$ . By comparing the results of localization with the analytic calculation of the slope function (similar to what we did in Section.5.3), it was possible to obtain an expression for the interpolation function for ABJM theory [32] and for a more general ABJ theory [33]. The detailed proof of these expressions is still an open question and would likely require the QSC formulation for the cusped Wilson-line in these theories, which is not known yet.

**QSC for Wilson Line with a Cusp** The anomalous dimension for the Maldacena-Wilson line with a cusp was shown to be integrable in [35, 34]. In [15] the QSC construction for this observable was formulated, which allowed for the precise numerical analysis and non-perturbative analytic results. In [16] by taking an appropriate limit of the cusp anomalous dimension, the potential between heavy quark–anti-quarks was studied in detail with the help of QSC.

**QSC for High Order Perturbative Expansion** The QSC method allows for a very efficient analytic perturbative expansion. A very nice and powerful method for  $sl(2)$  sector was developed in [37] allowing the computation of 10-loops analytical coefficients on a standard laptop in just 3 hours. An alternative method, which can be applied in general situation was developed in [14]. In [55] the project of creating a database perturbative expansion of low lying anomalous dimensions was initiated.

**QSC for QCD Pomeron** As we discuss in the Section 5.2 the QSC enables a very simple analytic continuation in the quantum numbers such as Lorentz spin  $S$ . As was explained in [38] one can approach the regime, where  $\mathcal{N} = 4$  SYM becomes similar to QCD. This regime can be also studied with the QSC [40]. In particular the most complicated highest transcendentality parts of the planar QCD result at 3 loops was obtained for the first time in [14], by using the QSC. It was later confirmed by an independent calculation in [39].

**QSC for Deformations of  $\mathcal{N} = 4$  SYM** The  $\mathcal{N} = 4$  admits numerous deformations. Some of them are analogous to the twists we discussed in Section 2.2 and can be easily introduced into the QSC formalism simply by modifying the asymptotic of the Q-functions. For some examples see [15, 31]. Another deformation is called  $\eta$ -deformation [36], which most likely can be described by the QSC as well, by replacing a simple cut in  $\mathbf{P}_a$  function with a periodised set of cuts<sup>1</sup>.

**QSC for Fishnet Graphs** In the limit when one of the twist parameters becomes large and the 't Hooft coupling simultaneously scales to zero one gets a significant simplification in the perturbation theory, which gets dominated by the “fishnet” scalar graphs. First this limit was considered for the cusp anomalous dimension in [34, 41] and it was possible to reproduce the result analytically from the QSC. A more systematic study of the “fishnet” limit of  $\mathcal{N} = 4$  was initiated by [42] where it was demonstrated that many more observables can be studied by considering a special type of diagram. In [43] it was shown how the QSC methods can be used to evaluate these type of Feynman graphs.

**Open Questions** Even though a number of longstanding problems were resolved with the help of the QSC there are still a number of open questions which could potentially be solved using the QSC. Some of them are likely to be solved soon, others may never be solved. Below we give an incomplete list of such problems, focusing on those more likely to be solved before the next ice age.

It would be very useful to be able to extract the strong coupling expansion of the spectrum analytically from the QSC. Some first steps were done in [44].

The structure of the QSC is very constraining and at the moment we only know two QSCs for SYM and ABJ(M). It would be useful to make a complete classification of the QSCs starting from the symmetry group. This way one should find the QSC for  $AdS_3/CFT_2$  and also possibly for a mysterious 6D theory – a mother theory of 6D integrable fishnet graphs. Similarly, different asymptotic and gluing conditions represent different observables in  $\mathcal{N} = 4$  SYM, it would be useful to have complete classification of such asymptotics and gluing conditions. For even more mathematically oriented readers there is the question of proving existence/countability of the solution of the QSC.

A big open conceptual question is how to derive the QSC from the gauge theory perspective, without a reference to AdS/CFT correspondence as this would allow us

---

<sup>1</sup>this case was considered very recently in [56].

to prove to some extent AdS/CFT by taking the classical limit of the QSC, deriving the Green-Schwartz classical spectral curve.

Some of the problems which are within immediate reach include: studying oderon dimension in the way similar to BFKL pomeron [14] (see for settings [52]); constructing the QSC for the recently proposed integrability framework for the Hagedorn phase transition [45] which would enable analytic weak coupling expansion and numerical analysis for this observable; integrable boundary problems with non-diagonal twist, like recently considered in [46] could be most likely treated in the way similar to [16], this problem seems to be also related to the problem of finding the spectrum of tachyons [47], which is another problem where the QSC reformulation could help to advance further.

A more complicated but very important problem is to extend the QSC formalism to the problem of computing n-point correlation function. Existing beautiful integrability-based hexagon formalism [48] should give important hints on resumming wrapping corrections. This problem seems to be linked to the problem of finding separated variables in the AdS/CFT for some first steps at weak coupling see [49]. The one-point function [51] could be the perfect framework for developing the new QSC-based formalism for the correlators. See also [50] for more exotic observables which could be also potentially governed by integrability.

Finally, the other main open questions are whether we could also use integrability to get non-planar corrections and also get closer to the real world QCD.

If you have questions, please feel free to email to [nikgromov@gmail.com](mailto:nikgromov@gmail.com). You are also welcome to email any answers to the above questions to [nickgromov@mail.ru](mailto:nickgromov@mail.ru)!



# Bibliography

1. N. Gromov and P. Vieira, “The AdS(5) x S\*\*5 superstring quantum spectrum from the algebraic curve,” Nucl. Phys. B **789** (2008) 175  
doi:10.1016/j.nuclphysb.2007.07.032 [hep-th/0703191 [HEP-TH]].
2. N. Gromov, V. Kazakov and P. Vieira, “Exact Spectrum of Anomalous Dimensions of Planar N=4 Supersymmetric Yang-Mills Theory,” Phys. Rev. Lett. **103** (2009) 131601 doi:10.1103/PhysRevLett.103.131601 [arXiv:0901.3753 [hep-th]].
3. N. Gromov, V. Kazakov, A. Kozak and P. Vieira, “Exact Spectrum of Anomalous Dimensions of Planar N = 4 Supersymmetric Yang-Mills Theory: TBA and excited states,” Lett. Math. Phys. **91** (2010) 265 doi:10.1007/s11005-010-0374-8 [arXiv:0902.4458 [hep-th]].
4. N. Gromov, V. Kazakov and P. Vieira, “Exact Spectrum of Planar  $\mathcal{N} = 4$  Supersymmetric Yang-Mills Theory: Konishi Dimension at Any Coupling,” Phys. Rev. Lett. **104** (2010) 211601 doi:10.1103/PhysRevLett.104.211601 [arXiv:0906.4240 [hep-th]].
5. N. Gromov, “Y-system and Quasi-Classical Strings,” JHEP **1001** (2010) 112 doi:10.1007/JHEP01(2010)112 [arXiv:0910.3608 [hep-th]].
6. N. Beisert *et al.*, “Review of AdS/CFT Integrability: An Overview,” Lett. Math. Phys. **99**, 3 (2012) doi:10.1007/s11005-011-0529-2 [arXiv:1012.3982 [hep-th]].
7. N. Gromov, V. Kazakov, S. Leurent and D. Volin, “Solving the AdS/CFT Y-system,” JHEP **1207**, 023 (2012) doi:10.1007/JHEP07(2012)023 [arXiv:1110.0562 [hep-th]].
8. N. Gromov, V. Kazakov, S. Leurent and D. Volin, “Quantum Spectral Curve for Planar  $\mathcal{N} = 4$  Super-Yang-Mills Theory,” Phys. Rev. Lett. **112**, no. 1, 011602 (2014) doi:10.1103/PhysRevLett.112.011602 [arXiv:1305.1939 [hep-th]].
9. N. Gromov, F. Levkovich-Maslyuk, G. Sizov and S. Valatka, “Quantum spectral curve at work: from small spin to strong coupling in  $\mathcal{N} = 4$  SYM,” JHEP **1407**, 156 (2014) doi:10.1007/JHEP07(2014)156 [arXiv:1402.0871 [hep-th]].
10. A. Cavaglià, D. Fioravanti, N. Gromov and R. Tateo, “Quantum Spectral Curve of the  $\mathcal{N} = 6$  Supersymmetric Chern-Simons Theory,” Phys. Rev. Lett. **113**, no. 2, 021601 (2014) doi:10.1103/PhysRevLett.113.021601 [arXiv:1403.1859 [hep-th]].
11. N. Gromov, V. Kazakov, S. Leurent and D. Volin, “Quantum spectral curve for arbitrary state/operator in AdS<sub>5</sub>/CFT<sub>4</sub>,” JHEP **1509**, 187 (2015)

- doi:10.1007/JHEP09(2015)187 [arXiv:1405.4857 [hep-th]].
12. M. Alfimov, N. Gromov and V. Kazakov, “QCD Pomeron from AdS/CFT Quantum Spectral Curve,” JHEP **1507**, 164 (2015) doi:10.1007/JHEP07(2015)164 [arXiv:1408.2530 [hep-th]].
  13. N. Gromov, F. Levkovich-Maslyuk and G. Sizov, “Quantum Spectral Curve and the Numerical Solution of the Spectral Problem in AdS<sub>5</sub>/CFT<sub>4</sub>,” JHEP **1606**, 036 (2016) doi:10.1007/JHEP06(2016)036 [arXiv:1504.06640 [hep-th]].
  14. N. Gromov, F. Levkovich-Maslyuk and G. Sizov, “Pomeron Eigenvalue at Three Loops in  $\mathcal{N} = 4$  Supersymmetric Yang-Mills Theory,” Phys. Rev. Lett. **115**, no. 25, 251601 (2015) doi:10.1103/PhysRevLett.115.251601 [arXiv:1507.04010 [hep-th]].
  15. N. Gromov and F. Levkovich-Maslyuk, “Quantum Spectral Curve for a cusped Wilson line in  $\mathcal{N} = 4$  SYM,” JHEP **1604**, 134 (2016) doi:10.1007/JHEP04(2016)134 [arXiv:1510.02098 [hep-th]].
  16. N. Gromov and F. Levkovich-Maslyuk, “Quark-anti-quark potential in  $\mathcal{N} = 4$  SYM,” JHEP **1612**, 122 (2016) doi:10.1007/JHEP12(2016)122 [arXiv:1601.05679 [hep-th]].
  17. D. Bombardelli, A. Cavaglià, D. Fioravanti, N. Gromov and R. Tateo, “The full Quantum Spectral Curve for  $AdS_4/CFT_3$ ,” arXiv:1701.00473 [hep-th].
  18. D. Bombardelli *et al.*, “An integrability primer for the gauge-gravity correspondence: An introduction,” J. Phys. A **49** (2016) no.32, 320301 doi:10.1088/1751-8113/49/32/320301 [arXiv:1606.02945 [hep-th]].
  19. N. Beisert, “The SU(2—2) dynamic S-matrix,” Adv. Theor. Math. Phys. **12** (2008) 945 doi:10.4310/ATMP.2008.v12.n5.a1 [hep-th/0511082].
  20. R. A. Janik, “The AdS(5) x S<sup>5</sup> superstring worldsheet S-matrix and crossing symmetry,” Phys. Rev. D **73**, 086006 (2006) doi:10.1103/PhysRevD.73.086006 [hep-th/0603038].
  21. N. Beisert, B. Eden and M. Staudacher, “Transcendentality and Crossing,” J. Stat. Mech. **0701**, P01021 (2007) doi:10.1088/1742-5468/2007/01/P01021 [hep-th/0610251].
  22. J. Ambjorn, R. A. Janik and C. Kristjansen, “Wrapping interactions and a new source of corrections to the spin-chain/string duality,” Nucl. Phys. B **736** (2006) 288 doi:10.1016/j.nuclphysb.2005.12.007 [hep-th/0510171].
  23. A. Cavaglia, D. Fioravanti and R. Tateo, “Extended Y-system for the  $AdS_5/CFT_4$  correspondence,” Nucl. Phys. B **843** (2011) 302 doi:10.1016/j.nuclphysb.2010.09.015 [arXiv:1005.3016 [hep-th]].
  24. D. Bombardelli, D. Fioravanti and R. Tateo, “Thermodynamic Bethe Ansatz for planar AdS/CFT: A Proposal,” J. Phys. A **42** (2009) 375401 doi:10.1088/1751-8113/42/37/375401 [arXiv:0902.3930 [hep-th]].
  25. G. Arutyunov and S. Frolov, “Thermodynamic Bethe Ansatz for the AdS(5) x S(5) Mirror Model,” JHEP **0905**, 068 (2009) doi:10.1088/1126-6708/2009/05/068 [arXiv:0903.0141 [hep-th]].
  26. J. Balog and A. Hegedus, “Hybrid-NLIE for the AdS/CFT spectral problem,” JHEP **1208**, 022 (2012) doi:10.1007/JHEP08(2012)022 [arXiv:1202.3244 [hep-th]].
  27. L. D. Faddeev, “How algebraic Bethe ansatz works for integrable model,” hep-th/9605187.

28. P. P. Kulish and N. Y. Reshetikhin, “Diagonalization Of  $Gl(n)$  Invariant Transfer Matrices And Quantum N Wave System (lee Model),” *J. Phys. A* **16** (1983) L591. doi:10.1088/0305-4470/16/16/001
29. B. Basso, “An exact slope for AdS/CFT,” arXiv:1109.3154 [hep-th].
30. N. Dorey and B. Vicedo, “On the dynamics of finite-gap solutions in classical string theory,” *JHEP* **0607**, 014 (2006) doi:10.1088/1126-6708/2006/07/014 [hep-th/0601194].
31. V. Kazakov, S. Leurent and D. Volin, “T-system on T-hook: Grassmannian Solution and Twisted Quantum Spectral Curve,” *JHEP* **1612**, 044 (2016) doi:10.1007/JHEP12(2016)044 [arXiv:1510.02100 [hep-th]].
32. A. Cavaglià, N. Gromov and F. Levkovich-Maslyuk, “On the Exact Interpolating Function in ABJ Theory,” *JHEP* **1612**, 086 (2016) doi:10.1007/JHEP12(2016)086 [arXiv:1605.04888 [hep-th]].
33. N. Gromov and G. Sizov, “Exact Slope and Interpolating Functions in  $N=6$  Supersymmetric Chern-Simons Theory,” *Phys. Rev. Lett.* **113** (2014) no.12, 121601 doi:10.1103/PhysRevLett.113.121601 [arXiv:1403.1894 [hep-th]].
34. D. Correa, J. Maldacena and A. Sever, “The quark anti-quark potential and the cusp anomalous dimension from a TBA equation,” *JHEP* **1208**, 134 (2012) doi:10.1007/JHEP08(2012)134 [arXiv:1203.1913 [hep-th]].
35. N. Drukker, “Integrable Wilson loops,” *JHEP* **1310** (2013) 135 doi:10.1007/JHEP10(2013)135 [arXiv:1203.1617 [hep-th]].
36. G. Arutyunov, R. Borsato and S. Frolov, “S-matrix for strings on  $\eta$ -deformed  $AdS_5 \times S^5$ ,” *JHEP* **1404** (2014) 002 doi:10.1007/JHEP04(2014)002 [arXiv:1312.3542 [hep-th]].
37. C. Marboe and D. Volin, “Quantum spectral curve as a tool for a perturbative quantum field theory,” *Nucl. Phys. B* **899** (2015) 810 doi:10.1016/j.nuclphysb.2015.08.021 [arXiv:1411.4758 [hep-th]].
38. A. V. Kotikov, L. N. Lipatov, A. Rej, M. Staudacher and V. N. Velizhanin, “Dressing and wrapping,” *J. Stat. Mech.* **0710**, P10003 (2007) doi:10.1088/1742-5468/2007/10/P10003 [arXiv:0704.3586 [hep-th]].
39. S. Caron-Huot and M. Herranen, “High-energy evolution to three loops,” arXiv:1604.07417 [hep-ph].
40. M. Alfimov, N. Gromov and V. Kazakov, “QCD Pomeron from AdS/CFT Quantum Spectral Curve,” *JHEP* **1507**, 164 (2015) doi:10.1007/JHEP07(2015)164 [arXiv:1408.2530 [hep-th]].
41. J. K. Erickson, G. W. Semenoff, R. J. Szabo and K. Zarembo, “Static potential in  $N=4$  supersymmetric Yang-Mills theory,” *Phys. Rev. D* **61** (2000) 105006 doi:10.1103/PhysRevD.61.105006 [hep-th/9911088].
42. Ö. Gürdoğan and V. Kazakov, “New Integrable 4D Quantum Field Theories from Strongly Deformed Planar  $\mathcal{N} = 4$  Supersymmetric Yang-Mills Theory,” *Phys. Rev. Lett.* **117** (2016) no.20, 201602 Addendum: [Phys. Rev. Lett. **117** (2016) no.25, 259903] doi:10.1103/PhysRevLett.117.201602, 10.1103/PhysRevLett.117.259903 [arXiv:1512.06704 [hep-th]].
43. N. Gromov, V. Kazakov, G. Korchemsky, S. Negro and G. Sizov, “Integrability of Conformal Fishnet Theory,” arXiv:1706.04167 [hep-th].

44. Á. Hegedűs and J. Konczer, “Strong coupling results in the  $AdS_5 /CF T_4$  correspondence from the numerical solution of the quantum spectral curve,” JHEP **1608** (2016) 061 doi:10.1007/JHEP08(2016)061 [arXiv:1604.02346 [hep-th]].
45. T. Harmark and M. Wilhelm, “The Hagedorn temperature of  $AdS_5/CFT_4$  via integrability,” arXiv:1706.03074 [hep-th].
46. M. Guica, F. Levkovich-Maslyuk and K. Zarembo, “Integrability in dipole-deformed  $N=4$  super Yang-Mills,” arXiv:1706.07957 [hep-th].
47. Z. Bajnok, N. Drukker, Á. Hegedűs, R. I. Nepomechie, L. Palla, C. Sieg and R. Suzuki, “The spectrum of tachyons in  $AdS/CFT$ ,” JHEP **1403**, 055 (2014) doi:10.1007/JHEP03(2014)055 [arXiv:1312.3900 [hep-th]].
48. B. Basso, S. Komatsu and P. Vieira, arXiv:1505.06745 [hep-th].
49. N. Gromov, F. Levkovich-Maslyuk and G. Sizov, arXiv:1610.08032 [hep-th].
50. I. Buhl-Mortensen, M. de Leeuw, A. C. Ipsen, C. Kristjansen and M. Wilhelm, “Asymptotic one-point functions in  $AdS/dCFT$ ,” arXiv:1704.07386 [hep-th].
51. I. Buhl-Mortensen, M. de Leeuw, C. Kristjansen and K. Zarembo, “One-point Functions in  $AdS/dCFT$  from Matrix Product States,” JHEP **1602** (2016) 052 doi:10.1007/JHEP02(2016)052 [arXiv:1512.02532 [hep-th]].
52. R. C. Brower, M. S. Costa, M. Djurić, T. Raben and C. I. Tan, “Strong Coupling Expansion for the Conformal Pomeron/Odderon Trajectories,” JHEP **1502** (2015) 104 doi:10.1007/JHEP02(2015)104 [arXiv:1409.2730 [hep-th]].
53. A. Cavaglià, M. Cornagliotto, M. Mattelliano and R. Tateo, “A Riemann-Hilbert formulation for the finite temperature Hubbard model,” JHEP **1506** (2015) 015 doi:10.1007/JHEP06(2015)015 [arXiv:1501.04651 [hep-th]].
54. M. Alfimov, N. Gromov, G. Sizov to appear.
55. C. Marboe and D. Volin, “The full spectrum of  $AdS_5/CFT_4$  I: Representation theory and one-loop Q-system,” arXiv:1701.03704 [hep-th].
56. R. Klabbers and S. J. van Tongeren, “Quantum Spectral Curve for the eta-deformed  $AdS_5 \times S^5$  superstring,” arXiv:1708.02894 [hep-th].